

# Parametric Bilinear Generalized Approximate Message Passing

Jason T. Parker, Yan Shou, and Philip Schniter

**Abstract**—We propose a scheme to estimate the parameters  $b_i$  and  $c_j$  of the bilinear form  $z_m = \sum_{i,j} b_i z_m^{(i,j)} c_j$  from noisy measurements  $\{y_m\}_{m=1}^M$ , where  $y_m$  and  $z_m$  are related through an arbitrary likelihood function and  $z_m^{(i,j)}$  are known. Our scheme is based on generalized approximate message passing (G-AMP): it treats  $b_i$  and  $c_j$  as random variables and  $z_m^{(i,j)}$  as an i.i.d. Gaussian tensor in order to derive a tractable simplification of the sum-product algorithm in the large-system limit. It generalizes previous instances of bilinear G-AMP, such as those that estimate matrices  $B$  and  $C$  from a noisy measurement of  $Z = BC$ , allowing the application of AMP methods to problems such as self-calibration, blind deconvolution, and matrix compressive sensing. Numerical experiments confirm the accuracy and computational efficiency of the proposed approach.

## I. INTRODUCTION

### A. Motivation

Many problems in engineering, science, and finance can be formulated as the estimation of a structured matrix  $Z \in \mathbb{R}^{M \times L}$  from a noisy (or otherwise corrupted) observation  $Y \in \mathbb{R}^{M \times L}$ . For various types of structure, the problem reduces to a well-known specialized problem. For example, when  $Z$  has a low-rank structure and only a subset of its entries are observed (possibly in noise), the estimation of  $Z$  is known as *matrix completion* (MC) [2]. When  $Z = L + S$  for low-rank  $L$  and sparse  $S$ , the estimation of  $L$  and  $S$  from a (noisy) observation of  $Z$  is known as *robust principal components analysis* (RPCA) [3], [4] or *stable principle components pursuit* (SPCP) [5]. When  $Z = BC$  with sparse  $C$ , the problem of estimating  $B$  and  $C$  from a (noisy) observation of  $Z$  is known as *dictionary learning* (DL) [6]. When  $Z = BC$  and both  $B$  and  $C$  are positive, the problem of estimating  $B, C$  from a (noisy) observation of  $Z$  is known as *nonnegative matrix factorization* (NMF) [7].

In this paper, we propose an AMP-based approach to a more general class of structured-matrix estimation problems. Our work is motivated by problems like the following.

- 1) Estimate  $b$  and  $C$  from a noisy observation of<sup>1</sup>

$$Z = \text{Diag}(Hb)AC \quad (1)$$

with known  $H$  and  $A$ . This problem manifests, e.g., in

- *Self-calibration* [8]. Here the columns of  $C$  are measured through a linear system, represented by the matrix  $A$ , whose outputs are subject to unknown (but structured) gains of the form  $Hb$ . The goal is to simultaneously recover the signal  $C$  and the calibration parameters  $b$ .
- *Blind circular deconvolution*: Here the columns of  $C$  are circularly convolved with the channel  $b$ , and the goal is to simultaneously recover  $C$  and  $b$  from a noisy version of the Fourier-domain convolution outputs.<sup>2</sup>

- 2) Consider the more general<sup>3</sup> problem of estimating  $\{b_i\}$  and  $C$  from a noisy observation of

$$Z = \sum_i b_i A^{(i)} C \quad (2)$$

with known  $\{A^{(i)}\}$ . This problem manifests, e.g., in

- *Compressive sensing with matrix uncertainty* [9]. Here,  $Z = AC$  where  $A = \sum_i b_i A^{(i)}$  is an unknown (but structured) sensing matrix and the columns of  $C \in \mathbb{R}^{N \times L}$  are sparse signals. The goal is to simultaneously recover  $C$  and the matrix uncertainty parameters  $\{b_i\}$ .
- *Joint channel-symbol estimation*. Say a symbol stream  $\{c_i\}$  is transmitted through a length- $N_b$  convolutive channel  $\{b_i\}$ , where the same length- $N_g \geq N_b - 1$  guard interval is repeated every  $N_p$  samples in  $\{c_i\}$ . Then the noiseless convolution outputs can be written as  $Z = \sum_i b_i A^{(i)} C$ , where  $A^{(i)} = [\mathbf{0}_{N_p \times (N_g - i + 1)} \quad \mathbf{I}_{N_p} \quad \mathbf{0}_{N_p \times (i - 1)}]$  and where the first and last  $N_g$  rows in  $C$  are guard symbols. The goal is to jointly estimate the channel  $\{b_i\}$  and the (finite-alphabet) data symbols in  $C$ .

- 3) Consider the yet more general<sup>4</sup> problem of estimating low-rank  $L$  and sparse  $S$  from noisy observations of

$$z_m = \text{tr}\{\Phi_m^T (L + S)\} \text{ for } m = 1, \dots, N_z \quad (3)$$

J. Parker is with the Air Force Research Laboratory, Dayton, OH 45433, e-mail: jason.parker.13@us.af.mil. His work on this project has been supported by AFOSR Lab Task 11RY02COR.

P. Schniter and Y. Shou are with the Dept. ECE, The Ohio State University, 2015 Neil Ave., Columbus OH 43210, e-mail: schniter@ece.osu.edu and shou.3@osu.edu, phone 614.247.6488, fax 614.292.7596. Their work on this project has been supported by NSF grants IIP-0968910, CCF-1018368, CCF-1218754, and by an allocation of computing time from the Ohio Supercomputer Center.

Portions of this work appeared in [1] and were presented at the Information Theory and Applications Workshop, La Jolla, CA, USA, February 2015.

<sup>1</sup>For clarity, we typeset matrices in bold capital, vectors in bold lowercase, and scalars in non-bold. Furthermore, we typeset random variables in sans-serif font (e.g.,  $\mathbf{Z}$ ) and deterministic realizations in serif font (e.g.,  $\mathbf{Z}$ ).

<sup>2</sup>Recall that circular convolution between  $b$  and  $c_l$  can be written as  $v_l = \text{Circ}(b)c_l$ , with circulant matrix  $\text{Circ}(b) = A^H \text{Diag}(\sqrt{N}Ab)A$  for unitary discrete Fourier transform (DFT) matrix  $A$ . The DFT of the convolution outputs is then  $Av_l = \text{Diag}(\sqrt{N}Ab)Ac_l$ , matching (1).

<sup>3</sup>Note (1) is a special case of (2) with  $A^{(i)} = \text{Diag}(h_i)A$ , where  $h_i$  denotes the  $i$ th column of  $H$ .

<sup>4</sup>[10] shows that (2) is a special case of (3) with rank-one  $L$  and  $S = \mathbf{0}$ .

with known  $\{\Phi_m\}$ . This problem is sometimes known as *matrix compressive sensing* (MCS), which has applications in, e.g., video surveillance [11], hyperspectral imaging [11], quantum state tomography [12], multi-task regression [13], and image processing [14].

### B. Approach

To solve structured-matrix estimation problems like those above, we start with a noiseless model of the form

$$\mathbf{z} = \sum_{i=0}^{N_b} \sum_{j=0}^{N_c} b_i \mathbf{z}^{(i,j)} c_j \in \mathbb{R}^M, \quad (4)$$

where  $\{\mathbf{z}^{(i,j)}\}$ ,  $b_0 = 1/\sqrt{N_b}$ , and  $c_0 = 1/\sqrt{N_c}$  are known. We then estimate the parameters  $\mathbf{b} = [b_1, \dots, b_{N_b}]^T$  and  $\mathbf{c} = [c_1, \dots, c_{N_c}]^T$  from  $\mathbf{y}$ , a “noisy” observation of  $\mathbf{z}$ . In doing so, we treat  $\mathbf{b}$  and  $\mathbf{c}$  as realizations of random vectors  $\mathbf{b}$  and  $\mathbf{c}$  with independent components, i.e.,

$$p_{\mathbf{b}, \mathbf{c}}(\mathbf{b}, \mathbf{c}) = \prod_{i=1}^{N_b} p_{b_i}(b_i) \prod_{j=1}^{N_c} p_{c_j}(c_j), \quad (5)$$

and we assume that the likelihood function of  $\mathbf{z}$  takes the separable form

$$p_{\mathbf{y}|\mathbf{z}}(\mathbf{y}|\mathbf{z}) = \prod_{m=1}^M p_{y_m|\mathbf{z}_m}(y_m|\mathbf{z}_m). \quad (6)$$

Note that our definition of “noisy” is quite broad due to the generality of  $p_{y_m|\mathbf{z}_m}$ . For example, (6) facilitates both additive noise and nonlinear measurement models like those arising with, e.g., quantization [15], Poisson noise [16], and phase retrieval [17]. Note also that, since  $b_0$  and  $c_0$  are known, the model (4) includes bilinear, linear, and constant terms. In Section IV, we demonstrate how (4)–(6) can be instantiated to solve various structured-matrix estimation problems.

Our estimation algorithm is based on the AMP framework [18]. Previously, AMP was applied to the *generalized linear* estimation problem: “estimate i.i.d.  $\mathbf{c}$  from  $\mathbf{y}$ , a noisy realization of  $\mathbf{z} = \mathbf{A}\mathbf{c}$ ,” leading to the G-AMP algorithm [19], and the *generalized bilinear* estimation problem: “estimate i.i.d.  $\mathbf{B}$  and  $\mathbf{C}$  from  $\mathbf{Y}$ , a noisy realization of  $\mathbf{Z} = \mathbf{B}\mathbf{C}$ ,” leading to the BiG-AMP algorithm [20]–[22]. In this paper, we apply AMP to estimate  $\{b_i\}$  and  $\{c_j\}$  in the *parametric bilinear* model (4), and we refer to the resulting algorithm as *Parametric BiG-AMP* (P-BiG-AMP).

We also show that, using an expectation-maximization (EM) [23] approach similar to those used in other AMP-based works [24]–[26], we can generalize our approach to the case where the parameters governing the distributions  $p_{b_i}$ ,  $p_{c_j}$ , and  $p_{y_m|\mathbf{z}_m}$  are unknown.

### C. Relation to Previous Work

We now describe related literature, starting with versions of compressive sensing (CS) under sensing-matrix uncertainty.

Consider first the problem of multiple measurement vector (MMV) CS with *output gain* uncertainty, i.e., recovering  $\mathbf{C}$  with sparse columns from a noisy observation of  $\mathbf{Z} = \text{Diag}(\mathbf{b})\mathbf{A}\mathbf{C}$ , where  $\mathbf{A}$  is known and  $\mathbf{b}$  is unknown. For the case of positive  $\mathbf{b}$  and no noise, [27] proposed a convex approach based on  $\ell_1$  minimization, which was generalized to arbitrary  $\mathbf{b}$  in [28]. For MMSE estimation in the noisy case, a

G-AMP-based approach to the MMV version was proposed in [29], and G-AMP approaches to the single measurement vector (SMV) version with coded-symbol  $\mathbf{b}$  and constant-modulus  $\mathbf{b}$  were proposed in [30] and [17]. Our proposed P-BiG-AMP approach handles more general forms of matrix uncertainty than [17], [29], [30].

MMV CS with *input gain* uncertainty, i.e., recovering possibly-sparse  $\mathbf{C}$  from a noisy observation of  $\mathbf{Z} = \mathbf{A} \text{Diag}(\mathbf{b})\mathbf{C}$ , where  $\mathbf{A}$  is known and  $\mathbf{b}$  is unknown, was considered in [31]. There, G-AMP estimation of  $\mathbf{C}$  was alternated with EM estimation of  $\mathbf{b}$  using the EM-AMP framework from [26]. As such, [31] does not support a prior on  $\mathbf{b}$ .

A related problem is SMV CS with *subspace-structured* output gain uncertainty, i.e., recovering sparse  $\mathbf{c}$  from a noisy observation of  $\mathbf{z} = \text{Diag}(\mathbf{H}\mathbf{b})\mathbf{A}\mathbf{c}$  with known  $\mathbf{A}, \mathbf{H}$ . This problem is perhaps better known as *blind deconvolution* of sequences  $\mathbf{b}, \mathbf{c}$  when  $\mathbf{H}, \mathbf{A}$  are DFT matrices and  $\mathbf{z}$  is the DFT-domain noiseless measurement vector. Several convex approaches to blind deconvolution have been proposed using the “lifting” technique, which transforms the problem to that of recovering a rank-1 matrix  $\mathbf{L}$  from a (noisy) observation of  $z_m = \text{tr}\{\Phi_m^T \mathbf{L}\}$  for  $m = 1, \dots, M$ . For example, [32] proposed a convex relaxation that applies to linear convolution with sparse  $\mathbf{c}$ , [33] proposed a convex relaxation (with guarantees) that applies to circular convolution with non-sparse  $\mathbf{b}, \mathbf{c}$ , [8] proposed a convex relaxation (with guarantees) that applies to circular convolution with sparse  $\mathbf{c}$ , and [34] proposed alternating and greedy schemes for sparse  $\mathbf{b}, \mathbf{c}$ . Meanwhile, identifiability conditions were studied in [35], [36].

For (2), i.e., CS with *general* matrix uncertainty, [9] proposed an alternating minimization scheme and [37] showed that the problem can be convexified via lifting and then used that insight to study identifiability issues.

Finally, consider the *matrix CS* problem given by (3). For generic<sup>5</sup>  $\{\Phi_m\}$ , greedy schemes were proposed in [11] and [39] and convex ones in [12]–[14], [40].

The P-BiG-AMP approach that we propose in this work supports all of the above matrix-uncertain CS, blind deconvolution, and low-rank-plus-sparse recovery models. Moreover, it allows arbitrary priors on  $b_i$  and  $c_j$ , allowing the exploitation of (approximate) sparsity, constant-modulus structure, finite-alphabet structure, etc. Furthermore, it allows a generic likelihood function of the form (6), allowing non-linear measurement models like quantization, Poisson noise, phase-retrieval, etc. Although it is non-convex and comes with no performance guarantees, it attacks the MMSE problem directly, and the empirical results in Section V suggest that it offers better MSE recovery performance than recent convex relaxations while being computationally competitive (if not faster).

### D. Organization and Notation

The remainder of this manuscript is organized as follows. In Section II we present preliminary material on belief propagation and AMP, and in Section III we derive our P-BiG-AMP

<sup>5</sup>For the special case where each  $\Phi_m$  has a single unit-valued entry (i.e., noisy elements of  $\mathbf{L} + \mathbf{S}$  are directly observed), many more schemes have been proposed (e.g., [3], [4], [38]), including AMP-based schemes [20]–[22].

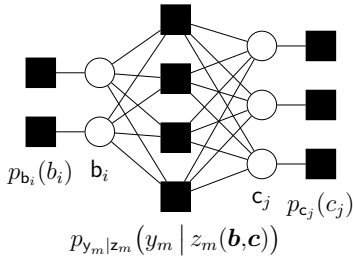


Fig. 1. The factor graph for parametric generalized bilinear inference under  $N_b = 2$ ,  $N_c = 3$ , and  $M = 4$ .

algorithm. In Section IV we show how the implementation of P-BiG-AMP can be simplified for several problems of interest, and in Section V we present the results of several numerical experiments. In Section VI, we conclude. Note that this manuscript is a shortened version of [10].

*Notation:* For random variable  $\mathbf{x}$ , we use  $p_{\mathbf{x}}(x)$  for the pdf,  $E\{\mathbf{x}\}$  for the mean, and  $\text{var}\{\mathbf{x}\}$  for the variance.  $\mathcal{N}(x; \hat{x}, \nu^x)$  denotes the Gaussian pdf with mean  $\hat{x}$  and variance  $\nu^x$ . For a matrix  $\mathbf{X}$ , we use  $\mathbf{x}_l = [\mathbf{X}]_{:,l}$  to denote the  $l^{\text{th}}$  column,  $x_{nl} = [\mathbf{X}]_{nl}$  to denote the entry in the  $n^{\text{th}}$  row and  $l^{\text{th}}$  column,  $\mathbf{X}^T$  the transpose,  $\mathbf{X}^*$  the conjugate,  $\mathbf{X}^H$  the conjugate transpose,  $\|\mathbf{X}\|_F$  the Frobenius norm, and  $\|\mathbf{X}\|_*$  the nuclear norm. For vectors  $\mathbf{x}$ , we use  $x_n = [\mathbf{x}]_n$  to denote the  $n^{\text{th}}$  entry and  $\|\mathbf{x}\|_p = (\sum_n |x_n|^p)^{1/p}$  to denote the  $\ell_p$  norm.  $\text{Diag}(\mathbf{x})$  is the diagonal matrix with diagonal elements  $\mathbf{x}$ ,  $\text{Conv}(\mathbf{x})$  is the convolution matrix with first column  $\mathbf{x}$ , and  $\text{Circ}(\mathbf{x})$  is the circular convolution matrix with first column  $\mathbf{x}$ .

## II. PRELIMINARIES

### A. Bayesian Inference

For the model defined by (4)-(6), the posterior pdf is

$$p_{\mathbf{b}, \mathbf{c} | \mathbf{y}}(\mathbf{b}, \mathbf{c} | \mathbf{y}) = p_{\mathbf{y} | \mathbf{b}, \mathbf{c}}(\mathbf{y} | \mathbf{b}, \mathbf{c}) p_{\mathbf{b}}(\mathbf{b}) p_{\mathbf{c}}(\mathbf{c}) / p_{\mathbf{y}}(\mathbf{y}) \quad (7)$$

$$\propto p_{\mathbf{y} | \mathbf{z}}(\mathbf{y} | \mathbf{z}(\mathbf{b}, \mathbf{c})) p_{\mathbf{b}}(\mathbf{b}) p_{\mathbf{c}}(\mathbf{c}) \quad (8)$$

$$= \prod_m p_{y_m | z_m}(y_m | z_m(\mathbf{b}, \mathbf{c})) \prod_i p_{b_i}(b_i) \prod_j p_{c_j}(c_j) \quad (9)$$

where (7) used Bayes' rule and  $\propto$  denotes equality up to a scale factor. This pdf can be represented using the bipartite factor graph shown in Fig. 1. There, the factors in (9) are represented by “factor nodes” appearing as black boxes and the random variables in (9) are represented by “variable nodes” appearing as white circles. Note that the observed data  $\{y_m\}$  are treated as parameters of the  $p_{y_m | z_m}(y_m | \cdot)$  factor nodes, and not as random variables. Although Fig. 1 shows an edge between every  $b_i$  and  $p_{y_m | z_m}$  node pair, the edge will vanish when  $z_m(\mathbf{b}, \mathbf{c})$  does not depend on  $b_i$ , and similar for  $c_j$ .

### B. Loopy Belief Propagation

Our goal is to compute minimum mean-squared error (MMSE) estimates of  $\mathbf{b}$  and  $\mathbf{c}$ , i.e., the means of the marginal posteriors  $p_{b_i | \mathbf{y}}(\cdot | \mathbf{y})$  and  $p_{c_j | \mathbf{y}}(\cdot | \mathbf{y})$ . Since exact computation is intractable in our problem (see below), we consider approximate computation using loopy belief propagation (LBP).

In LBP, beliefs about the random variables (in the form of pdfs or log pdfs) are propagated among the nodes of the factor

graph until they converge. The standard way to compute these beliefs, known as the *sum-product algorithm* (SPA) [41], [42], says that the belief emitted by a variable node along a given edge of the graph is computed as the product of the incoming beliefs from all other edges, whereas the belief emitted by a factor node along a given edge is computed as the integral of the product of the factor associated with that node and the incoming beliefs on all other edges. The product of all beliefs impinging on a given variable node yields the posterior pdf for that variable. In cases where the factor graph has no loops, exact marginal posteriors result from two (i.e., forward and backward) passes of the SPA [41], [42]. For loopy factor graphs like ours, exact inference is in general NP hard [43] and so LBP does not guarantee correct posteriors. However, it often gives good approximations [44].

### C. Sum-Product Algorithm

We formulate the SPA using the messages and log-posteriors specified in Table I. All take the form of log-pdfs with arbitrary constant offsets, which can be converted to pdfs via exponentiation and scaling.

Applying the SPA to the factor graph in Fig. 1, we arrive at the following update rules for the four messages in Table I:

$$\begin{aligned} \Delta_{m \rightarrow i}^b(t, b_i) &= \log \int_{\{b_r\}_{r \neq i}, \{c_k\}_{k=1}^{N_c}} p_{y_m | z_m}(y_m | z_m(\mathbf{b}, \mathbf{c})) \\ &\quad \times \prod_{r \neq i} \exp(\Delta_{m \leftarrow r}^b(t, b_r)) \prod_{k=1}^{N_c} \exp(\Delta_{m \leftarrow k}^c(t, c_k)) \\ &\quad + \text{const} \end{aligned} \quad (10)$$

$$\begin{aligned} \Delta_{m \rightarrow j}^c(t, c_j) &= \log \int_{\{b_r\}_{r=1}^{N_b}, \{c_k\}_{k \neq j}} p_{y_m | z_m}(y_m | z_m(\mathbf{b}, \mathbf{c})) \\ &\quad \times \prod_{r=1}^{N_b} \exp(\Delta_{m \leftarrow r}^b(t, b_r)) \prod_{k \neq j} \exp(\Delta_{m \leftarrow k}^c(t, c_k)) \\ &\quad + \text{const} \end{aligned} \quad (11)$$

$$\Delta_{m \leftarrow i}^b(t+1, b_i) = \log p_{b_i}(b_i) + \sum_{r \neq m} \Delta_{r \rightarrow i}^b(t, b_i) + \text{const} \quad (12)$$

$$\Delta_{m \leftarrow j}^c(t+1, c_j) = \log p_{c_j}(c_j) + \sum_{r \neq m} \Delta_{r \rightarrow j}^c(t, c_j) + \text{const}, \quad (13)$$

where **const** denotes a constant (w.r.t  $b_i$  in (10) and (12) and w.r.t  $c_j$  in (11) and (13)). In the sequel, we denote the mean and variance of the pdf  $\frac{1}{C} \exp(\Delta_{m \leftarrow i}^b(t, \cdot))$  by  $\hat{b}_{m,i}(t)$  and  $\nu_{m,i}^b(t)$ , respectively, and we denote the mean and variance of  $\frac{1}{C} \exp(\Delta_{m \leftarrow j}^c(t, \cdot))$  by  $\hat{c}_{m,j}(t)$  and  $\nu_{m,j}^c(t)$ . We refer to the vectors of these statistics for a given  $m$  as  $\hat{\mathbf{b}}_m(t), \boldsymbol{\nu}_m^b(t) \in \mathbb{R}^{N_b}$  and  $\hat{\mathbf{c}}_m(t), \boldsymbol{\nu}_m^c(t) \in \mathbb{R}^{N_c}$ . For the log-posteriors, the SPA implies

$$\Delta_i^b(t+1, b_i) = \log p_{b_i}(b_i) + \sum_m \Delta_{m \rightarrow i}^b(t, b_i) + \text{const} \quad (14)$$

$$\Delta_j^c(t+1, c_j) = \log p_{c_j}(c_j) + \sum_m \Delta_{m \rightarrow j}^c(t, c_j) + \text{const} \quad (15)$$

and we denote the mean and variance of  $\frac{1}{C} \exp(\Delta_i^b(t, \cdot))$  by  $\hat{b}_i(t)$  and  $\nu_i^b(t)$ , and the mean and variance of  $\frac{1}{C} \exp(\Delta_j^c(t, \cdot))$  by  $\hat{c}_j(t)$  and  $\nu_j^c(t)$ . Finally, we denote the vectors of these statistics as  $\hat{\mathbf{b}}(t), \boldsymbol{\nu}^b(t) \in \mathbb{R}^{N_b}$  and  $\hat{\mathbf{c}}(t), \boldsymbol{\nu}^c(t) \in \mathbb{R}^{N_c}$ .

### D. Approximate Message Passing

When the priors and/or likelihood are generic, as in our case, exact representation of the SPA messages becomes difficult, motivating SPA approximations. One such approximation

$\Delta_{m \rightarrow i}^b(t, \cdot)$	SPA message from node $p_{y_m z_m}$ to node $\mathbf{b}_i$
$\Delta_{m \leftarrow i}^b(t, \cdot)$	SPA message from node $\mathbf{b}_i$ to node $p_{y_m z_m}$
$\Delta_{m \rightarrow j}^c(t, \cdot)$	SPA message from node $p_{y_m z_m}$ to node $\mathbf{c}_j$
$\Delta_{m \leftarrow j}^c(t, \cdot)$	SPA message from node $\mathbf{c}_j$ to node $p_{y_m z_m}$
$\Delta_i^b(t, \cdot)$	SPA-approximated log posterior pdf of $\mathbf{b}_i$
$\Delta_j^c(t, \cdot)$	SPA-approximated log posterior pdf of $\mathbf{c}_j$

TABLE I  
SPA MESSAGE DEFINITIONS AT ITERATION  $t \in \mathbb{Z}$ .

technique, known as *approximate message passing* (AMP) [18], becomes applicable when the statistical model involves multiplication of the unknown vectors with large random matrices. In this case, central-limit-theorem (CLT) and Taylor-series arguments can be used to arrive at a tractable SPA approximation that can be rigorously analyzed [45]. In the sequel, we propose an AMP-based approximation of the SPA in Section II-C.

### III. PARAMETRIC BiG-AMP

We now derive the proposed AMP-based approximation of the SPA algorithm from Section II-C, which we refer to as P-BiG-AMP. Due to space constraints, some details are omitted. The full derivation can be found in [10].

#### A. Randomization and Large-System Limit

For the derivation of P-BiG-AMP, we treat  $z_m^{(i,j)}$  as realizations of i.i.d. zero-mean unit-variance Gaussian random variables  $\mathbf{z}_m^{(i,j)}$ , and we treat  $\mathbf{z}_m^{(i,j)}$ ,  $\mathbf{b}_i$ ,  $\mathbf{c}_j$  as independent for all  $m, i, j$ . Furthermore, we consider a large-system limit (LSL) where  $M, N_b, N_c \rightarrow \infty$  such that  $N_b/M$  and  $N_c/M$  converge to fixed positive constants. Without loss of generality (w.l.o.g.) we will assume that  $\mathbb{E}\{\mathbf{b}_i^2\}$  and  $\mathbb{E}\{\mathbf{c}_j^2\}$  scale as  $O(1/M)$ . Given these assumptions, it is straightforward to show from (4) that  $\mathbb{E}\{\mathbf{z}_m^2\}$  scales as  $O(1)$ .

To derive P-BiG-AMP, we will examine the SPA updates (10)-(15) and drop those terms that vanish in the LSL, i.e., as  $M \rightarrow \infty$ .

#### B. SPA message from node $p_{y_m|z_m}$ to node $\mathbf{b}_i$

We begin by approximating the message defined in (10). First, we invoke the LSL to apply the central limit theorem (CLT) to  $\mathbf{z}_m \triangleq z_m(\mathbf{b}, \mathbf{c})$ , where  $\mathbf{b}$  and  $\mathbf{c}$  are distributed according to the pdfs in (10). (Details on the application of the CLT are given in [10].) With the CLT, we can treat  $\mathbf{z}_m$  conditioned on  $\mathbf{b}_i = b_i$  as Gaussian and thus completely characterize it by a (conditional) mean and variance. In particular,

the conditional mean is

$$\mathbb{E}\{\mathbf{z}_m | \mathbf{b}_i = b_i\} = \mathbb{E}\left\{\sum_{k,j} \mathbf{b}_k \mathbf{c}_j z_m^{(k,j)} + (b_i - \mathbf{b}_i) \sum_j \mathbf{c}_j z_m^{(i,j)}\right\} \quad (16)$$

$$= \underbrace{\sum_{k,j} \hat{b}_{m,k}(t) \hat{c}_{m,j}(t) z_m^{(k,j)}}_{\triangleq \hat{z}_{\rightarrow m}^{(*,*)}(t)} + (b_i - \hat{b}_{m,i}(t)) \underbrace{\sum_j \hat{c}_{m,j}(t) z_m^{(i,j)}}_{\triangleq \hat{z}_{\rightarrow m}^{(i,*)}(t)} \quad (17)$$

$$= \underbrace{\hat{z}_{\rightarrow m}^{(*,*)}(t) - \hat{b}_{m,i}(t) \hat{z}_{\rightarrow m}^{(i,*)}(t)}_{\triangleq \hat{p}_{i,m}(t)} + b_i \hat{z}_{\rightarrow m}^{(i,*)}(t), \quad (18)$$

and it can be shown [10] that the conditional variance is

$$\text{var}\{\mathbf{z}_m | \mathbf{b}_i = b_i\} = \nu_{i,m}^p(t) + b_i^2 \sum_{j=1}^{N_c} \nu_{m,j}^c(t) z_m^{(i,j)2} + 2b_i \sum_{j=1}^{N_c} \nu_{m,j}^c(t) \left( \hat{z}_{\rightarrow m}^{(*,j)}(t) z_m^{(i,j)} - \hat{b}_{m,i}(t) z_m^{(i,j)2} \right), \quad (19)$$

for  $\hat{z}_{\rightarrow m}^{(*,j)}(t) \triangleq \sum_k \hat{b}_{m,k}(t) z_m^{(k,j)}$  and

$$\begin{aligned} \nu_{i,m}^p(t) &\triangleq \sum_{k \neq i} \nu_{m,k}^b(t) \left( \hat{z}_{\rightarrow m}^{(k,*)}(t)^2 + \sum_{j=1}^{N_c} \nu_{m,j}^c(t) z_m^{(k,j)2} \right) \\ &\quad + \sum_{j=1}^{N_c} \nu_{m,j}^c(t) \left( \hat{z}_{\rightarrow m}^{(*,j)}(t)^2 + \hat{b}_{m,i}(t)^2 z_m^{(i,j)2} \right. \\ &\quad \left. - 2\hat{b}_{m,i}(t) \hat{z}_{\rightarrow m}^{(*,j)}(t) z_m^{(i,j)} \right). \end{aligned} \quad (20)$$

The Gaussian approximation of  $\mathbf{z}_m | \mathbf{b}_i = b_i$  (with mean and variance above) can now be used to simplify the representation of the SPA message (10) from an  $(N_b + N_c - 1)$ -dimensional integral to a one-dimensional integral:

$$\Delta_{m \rightarrow i}^b(t, b_i) \approx \log \int_{z_m} p_{y_m|z_m}(y_m | z_m) \times \mathcal{N}(z_m; \mathbb{E}\{\mathbf{z}_m | \mathbf{b}_i = b_i\}, \text{var}\{\mathbf{z}_m | \mathbf{b}_i = b_i\}) \quad (21)$$

$$= H_m \left( \hat{p}_{i,m}(t) + b_i \hat{z}_{\rightarrow m}^{(i,*)}(t), \nu_{i,m}^p(t) + b_i^2 \sum_j \nu_{m,j}^c(t) z_m^{(i,j)2} + 2b_i \sum_{j=1}^{N_c} \nu_{m,j}^c(t) \left[ \hat{z}_{\rightarrow m}^{(*,j)}(t) z_m^{(i,j)} - \hat{b}_{m,i}(t) z_m^{(i,j)2} \right] \right) + \text{const}, \quad (22)$$

where we have introduced the shorthand notation

$$H_m(\hat{q}, \nu^q) \triangleq \log \int_z p_{y_m|z_m}(y_m | z) \mathcal{N}(z; \hat{q}, \nu^q). \quad (23)$$

We now further approximate (22). For this, we first introduce  $i$ -invariant versions of  $\hat{p}_{i,m}(t)$  and  $\nu_{i,m}^p(t)$ :

$$\hat{p}_m(t) \triangleq \hat{z}_{\rightarrow m}^{(*,*)}(t) \quad (24)$$

$$\begin{aligned} \nu_m^p(t) &\triangleq \sum_{j=1}^{N_c} \nu_{m,j}^c(t) \hat{z}_{\rightarrow m}^{(*,j)}(t)^2 + \sum_{k=1}^{N_b} \nu_{m,k}^b(t) \left[ \hat{z}_{\rightarrow m}^{(k,*)}(t)^2 \right. \\ &\quad \left. + \sum_{j=1}^{N_c} \nu_{m,j}^c(t) z_m^{(k,j)2} \right], \end{aligned} \quad (25)$$

noting that

$$\hat{p}_{m,i}(t) = \hat{p}_m(t) - \hat{b}_{m,i}(t) \hat{z}_{\rightarrow m}^{(i,*)}(t) \quad (26)$$

$$\begin{aligned} \nu_{i,m}^p(t) &= \nu_m^p(t) - \nu_{m,i}^b(t) \left[ \hat{z}_{\rightarrow m}^{(i,*)}(t)^2 + \sum_{j=1}^{N_c} \nu_{m,j}^c(t) z_m^{(i,j)2} \right] \\ &\quad + \sum_{j=1}^{N_c} \nu_{m,j}^c(t) \left[ \hat{b}_{m,i}(t)^2 z_m^{(i,j)2} - 2\hat{b}_{m,i}(t) \hat{z}_{\rightarrow m}^{(*,j)}(t) z_m^{(i,j)} \right]. \end{aligned} \quad (27)$$

Next, we define

$$\hat{z}_m^{(i,*)}(t) \triangleq \sum_j \hat{c}_j(t) z_m^{(i,j)} \quad (28)$$

$$\hat{z}_m^{(*,j)}(t) \triangleq \sum_i \hat{b}_i(t) z_m^{(i,j)} \quad (29)$$

$$\hat{z}_m^{(*,*)}(t) \triangleq \sum_{i,j} \hat{b}_i(t) \hat{c}_j(t) z_m^{(i,j)}, \quad (30)$$

which are versions of  $\hat{z}_{\rightarrow m}^{(i,*)}(t)$ ,  $\hat{z}_{\rightarrow m}^{(*,j)}(t)$ ,  $\hat{z}_{\rightarrow m}^{(*,*)}(t)$  evaluated at  $\hat{\mathbf{b}}(t)$  and  $\hat{\mathbf{c}}(t)$ , the means of the SPA-approximated posteriors, rather than at  $\hat{\mathbf{b}}_m(t)$  and  $\hat{\mathbf{c}}_m(t)$ , the means of the SPA messages. It can then be shown [10] that, with these new quantities, (22) can be expressed as

$$\begin{aligned} \Delta_{m \rightarrow i}^b(t, b_i) &= \text{const} \\ &+ H_m \left( \hat{p}_m(t) + (b_i - \hat{b}_i(t)) \hat{z}_{\rightarrow m}^{(i,*)}(t) + O(1/M), \right. \\ &\quad \left. \nu_m^p(t) + (b_i - \hat{b}_i(t))^2 \sum_{j=1}^{N_c} \nu_{m,j}^c(t) z_m^{(i,j)2} \right. \\ &\quad \left. + 2(b_i - \hat{b}_i(t)) \sum_{j=1}^{N_c} \nu_{m,j}^c(t) \hat{z}_m^{(*,j)}(t) z_m^{(i,j)} + O(1/M) \right). \end{aligned} \quad (31)$$

We will find it useful in the sequel to interpret  $\hat{z}_m^{(k,*)}(t)$ ,  $\hat{z}_m^{(*,j)}(t)$ ,  $z_m^{(i,j)}$  in (28)-(30) as partial derivatives:

$$\hat{z}_m^{(i,*)}(t) = \frac{\partial}{\partial b_i} z_m(\mathbf{b}, \mathbf{c}) \Big|_{\mathbf{b} = \hat{\mathbf{b}}(t), \mathbf{c} = \hat{\mathbf{c}}(t)} \quad (32)$$

$$\hat{z}_m^{(*,j)}(t) = \frac{\partial}{\partial c_j} z_m(\mathbf{b}, \mathbf{c}) \Big|_{\mathbf{b} = \hat{\mathbf{b}}(t), \mathbf{c} = \hat{\mathbf{c}}(t)} \quad (33)$$

$$z_m^{(i,j)} = \frac{\partial^2}{\partial b_i \partial c_j} z_m(\mathbf{b}, \mathbf{c}) \Big|_{\mathbf{b} = \hat{\mathbf{b}}(t), \mathbf{c} = \hat{\mathbf{c}}(t)}. \quad (34)$$

The next step is to perform a Taylor series expansion of (31) in  $b_i$  about  $\hat{b}_i(t)$ . By carefully analyzing the scaling of all terms in the expansion, and neglecting those that vanish as  $M \rightarrow \infty$ , it can be shown [10] that

$$\begin{aligned} \Delta_{m \rightarrow i}^b(t, b_i) &= \text{const} + \left[ \hat{s}_m(t) \hat{z}_{\rightarrow m}^{(i,*)}(t) + \nu_m^s(t) \hat{b}_i(t) \hat{z}_m^{(i,*)}(t)^2 \right. \\ &\quad \left. + (\hat{s}_m^2(t) - \nu_m^s(t)) \sum_j \nu_j^c(t) z_m^{(i,j)} (\hat{z}_m^{(*,j)}(t) - \hat{b}_i(t) z_m^{(i,j)}) \right] b_i \\ &\quad - \frac{1}{2} \left[ \nu_m^s(t) \hat{z}_m^{(i,*)}(t)^2 - (\hat{s}_m^2(t) - \nu_m^s(t)) \sum_j \nu_j^c(t) z_m^{(i,j)2} \right] b_i^2, \end{aligned} \quad (35)$$

using the definitions

$$\hat{s}_m(t) \triangleq H'_m(\hat{p}_m(t), \nu_m^p(t)) \quad (36)$$

$$\nu_m^s(t) \triangleq -H''_m(\hat{p}_m(t), \nu_m^p(t)), \quad (37)$$

where  $H'_m(\cdot, \cdot)$  and  $H''_m(\cdot, \cdot)$  respectively denote the first and second derivative w.r.t. the first argument of  $H_m(\cdot, \cdot)$ . Note that, since (35) is quadratic, the (exponentiated) message from  $p_{y_m|z_m}$  to  $\mathbf{b}_i$  is Gaussian in the LSL.

Furthermore, the derivation in [20, App. A] shows that (36)-(37) can be rewritten as

$$\hat{s}_m(t) = (\hat{z}_m(t) - \hat{p}_m(t)) / \nu_m^p(t) \quad (38)$$

$$\nu_m^s(t) = (1 - \nu_m^z(t) / \nu_m^p(t)) / \nu_m^p(t), \quad (39)$$

using the conditional mean and variance

$$\hat{z}_m(t) \triangleq \mathbb{E}\{Z_m | \mathbf{p}_m = \hat{\mathbf{p}}_m(t); \nu_m^p(t)\} \quad (40)$$

$$\nu_m^z(t) \triangleq \text{var}\{Z_m | \mathbf{p}_m = \hat{\mathbf{p}}_m(t); \nu_m^p(t)\}, \quad (41)$$

Note (40)-(41) are computed according to the pdf given in (D1) of Table II, which is P-BiG-AMP's iteration- $t$  approximation to the true marginal posterior  $p_{z_m|\mathbf{y}}(z_m|\mathbf{y})$ .

### C. SPA message from node $p_{y_m|z_m}$ to node $\mathbf{c}_j$

Since  $z_m = \sum_{i=0}^{N_b} \sum_{j=0}^{N_c} \mathbf{b}_i z_m^{(i,j)} \mathbf{c}_j$  implies a symmetry between  $\mathbf{b}_i$  and  $\mathbf{c}_j$ , the procedure to approximate  $\Delta_{m \rightarrow j}^c(t, \cdot)$  is essentially the same as that to approximate  $\Delta_{m \rightarrow i}^b(t, \cdot)$  from Section III-B. The end result is

$$\begin{aligned} \Delta_{m \rightarrow j}^c(t, c_j) &= \text{const} + \left[ \hat{s}_m(t) \hat{z}_{\rightarrow m}^{(*,j)}(t) + \nu_m^s(t) \hat{c}_j(t) \hat{z}_m^{(*,j)}(t)^2 \right. \\ &\quad \left. + (\hat{s}_m^2(t) - \nu_m^s(t)) \sum_i \nu_i^b(t) z_m^{(i,j)} (\hat{z}_m^{(i,*)}(t) - \hat{c}_j(t) z_m^{(i,j)}) \right] c_j \\ &\quad - \frac{1}{2} \left[ \nu_m^s(t) \hat{z}_m^{(*,j)}(t)^2 - (\hat{s}_m^2(t) - \nu_m^s(t)) \sum_i \nu_i^b(t) z_m^{(i,j)2} \right] c_j^2. \end{aligned} \quad (42)$$

### D. SPA message from node $\mathbf{c}_j$ to $p_{y_m|z_m}$

We now turn our attention to approximating the messages flowing out of the variable nodes. To start, we plug the approximation of  $\Delta_{m \rightarrow j}^c(t, c_j)$  from (42) into (13) and find

$$\begin{aligned} \Delta_{m \leftarrow j}^c(t+1, c_j) &\approx \text{const} + \log(p_{c_j}(c_j) \mathcal{N}(c_j; \hat{r}_{m,j}(t), \nu_{m,j}^r(t))) \end{aligned} \quad (43)$$

where

$$\begin{aligned} \nu_{m,j}^r(t) &\triangleq \left[ \sum_{r \neq m} \left( \nu_r^s(t) \hat{z}_r^{(*,j)}(t)^2 \right. \right. \\ &\quad \left. \left. - (\hat{s}_r^2(t) - \nu_r^s(t)) \sum_{i=1}^{N_b} \nu_i^b(t) z_r^{(i,j)2} \right) \right]^{-1} \end{aligned} \quad (44)$$

$$\begin{aligned} \hat{r}_{m,j}(t) &\triangleq \hat{c}_j(t) + \nu_{m,j}^r(t) \sum_{r \neq m} \left( (\hat{s}_r^2(t) - \nu_r^s(t)) \right. \\ &\quad \left. \times \sum_{i=1}^{N_b} \nu_i^b(t) z_r^{(i,j)} \hat{z}_r^{(i,*)}(t) + \hat{s}_r(t) \hat{z}_{\rightarrow r}^{(*,j)}(t) \right). \end{aligned} \quad (45)$$

The mean and variance of the pdf associated with the  $\Delta_{m \leftarrow j}^c(t+1, c_j)$  message approximation from (43) are

$$\begin{aligned} \hat{c}_{m,j}(t+1) &\triangleq \frac{1}{K} \int_c c p_{c_j}(c) \mathcal{N}(c; \hat{r}_{m,j}(t), \nu_{m,j}^r(t)) \\ &\triangleq g_{c_j}(\hat{r}_{m,j}(t), \nu_{m,j}^r(t)) \\ \nu_{m,j}^c(t+1) &\triangleq \frac{1}{K} \int_c |c - \hat{c}_{m,j}(t+1)|^2 p_{c_j}(c) \mathcal{N}(c; \hat{r}_{m,j}(t), \nu_{m,j}^r(t)) \\ &\triangleq \nu_{m,j}^r(t) g'_{c_j}(\hat{r}_{m,j}(t), \nu_{m,j}^r(t)) \end{aligned} \quad (46)$$

with  $K = \int_c p_{c_j}(c) \mathcal{N}(c; \hat{r}_{m,j}(t), \nu_{m,j}^r(t))$  and where  $g'_{c_j}$  denotes the derivative of  $g_{c_j}$  with respect to its first argument. The fact that (46) and (47) are related through a derivative was shown in [19].

Next we develop mean and variance approximations that do not depend on the destination node  $m$ . For this, we introduce  $m$ -invariant versions of  $\hat{r}_{m,j}(t)$  and  $\nu_{m,j}^r(t)$ :

$$\begin{aligned} \nu_j^r(t) &\triangleq \left[ \sum_m \left( \nu_m^s(t) \hat{z}_m^{(*,j)}(t)^2 \right. \right. \\ &\quad \left. \left. - (\hat{s}_m^2(t) - \nu_m^s(t)) \sum_{i=1}^{N_b} \nu_i^b(t) z_m^{(i,j)2} \right) \right]^{-1} \end{aligned} \quad (48)$$

$$\begin{aligned} \hat{r}_j(t) &\triangleq \hat{c}_j(t) + \nu_j^r(t) \sum_m \left( (\hat{s}_m^2(t) - \nu_m^s(t)) \right. \\ &\quad \left. \times \sum_{i=1}^{N_b} \nu_i^b(t) z_m^{(i,j)} \hat{z}_m^{(i,*)}(t) + \hat{s}_m(t) \hat{z}_{\rightarrow m}^{(*,j)}(t) \right). \end{aligned} \quad (49)$$

Comparing (44)-(45) to (48)-(49) reveals that  $(\nu_{m,j}^r(t) - \nu_j^r(t))$  scales as  $O(1/M^2)$  and that  $\hat{r}_{m,j}(t) = \hat{r}_j(t) -$

$\nu_j^r(t)\hat{s}_m(t)\hat{z}_m^{(*,j)}(t) + O(1/M^{3/2})$ , and thus (46) implies

$$\begin{aligned} & \hat{c}_{m,j}(t+1) \\ &= g_{c_j}(\hat{r}_j(t) - \nu_j^r(t)\hat{s}_m(t)\hat{z}_m^{(*,j)}(t) + O(1/M^{3/2}), \\ & \quad \nu_j^r(t) + O(1/M^2)) \end{aligned} \quad (50)$$

$$= g_{c_j}(\hat{r}_j(t) - \nu_j^r(t)\hat{s}_m(t)\hat{z}_m^{(*,j)}(t), \nu_j^r(t)) + O(1/M^{3/2}) \quad (51)$$

$$= g_{c_j}(\hat{r}_j(t), \nu_j^r(t)) \quad (52)$$

$$- \nu_j^r(t)g'_{c_j}(\hat{r}_j(t), \nu_j^r(t))\hat{s}_m(t)\hat{z}_m^{(*,j)}(t) + O(1/M^{3/2})$$

$$= \hat{c}_j(t+1) - \hat{s}_m(t)\hat{z}_m^{(*,j)}(t)\nu_j^c(t+1) + O(1/M^{3/2}), \quad (53)$$

where (51) follows by taking Taylor series expansions of (50) about the perturbations to the arguments; (52) follows by taking a Taylor series expansion of (51) in the first argument about the point  $\hat{r}_j(t)$ ; and (53) follows from the definitions

$$\hat{c}_j(t+1) \triangleq g_{c_j}(\hat{r}_j(t), \nu_j^r(t)) \quad (54)$$

$$\nu_j^c(t+1) \triangleq \nu_j^r(t)g'_{c_j}(\hat{r}_j(t), \nu_j^r(t)). \quad (55)$$

#### E. SPA message from node $b_i$ to $p_{y_m|z_m}$

Once again, due to symmetry, the derivation for  $\Delta_{m \leftarrow i}^b(t+1, b_i)$  closely parallels that for  $\Delta_{m \leftarrow j}^c(t+1, c_j)$ . Plugging approximation (35) into (12), we obtain

$$\begin{aligned} \Delta_{m \leftarrow i}^b(t+1, b_i) &\approx \log(p_{c_i}(b_i)\mathcal{N}(b_i; \hat{q}_{m,i}(t), \nu_{m,i}^q(t))) \\ &+ \text{const} \end{aligned} \quad (56)$$

$$\begin{aligned} \nu_{m,i}^q(t) &\triangleq \left[ \sum_{r \neq m} \left( \nu_r^s(t)\hat{z}_r^{(i,*)}(t)^2 \right. \right. \\ &\quad \left. \left. - (\hat{s}_r^2(t) - \nu_r^s(t)) \sum_{j=1}^{N_c} \nu_j^c(t)z_r^{(i,j)2} \right) \right]^{-1} \end{aligned} \quad (57)$$

$$\begin{aligned} \hat{q}_{m,i}(t) &\triangleq \hat{b}_i(t) + \nu_{m,i}^q(t) \sum_{r \neq m} \left( (\hat{s}_r^2(t) - \nu_r^s(t)) \right. \\ &\quad \left. \times \sum_{j=1}^{N_c} \nu_j^c(t)z_r^{(i,j)}\hat{z}_r^{(*,j)}(t) + \hat{s}_r(t)\hat{z}_{\rightarrow r}^{(i,*)}(t) \right). \end{aligned} \quad (58)$$

The mean and variance of the pdf associated with the  $\Delta_{m \leftarrow i}^b(t+1, b_i)$  approximation from (56) are then

$$\begin{aligned} \hat{b}_{m,i}(t+1) &\triangleq \frac{1}{K} \int_b b p_{b_i}(b) \mathcal{N}(b; \hat{q}_{m,i}(t), \nu_{m,i}^q(t)) \\ &\triangleq g_{b_i}(\hat{q}_{m,i}(t), \nu_{m,i}^q(t)) \\ \nu_{m,i}^b(t+1) &\triangleq \frac{1}{K} \int_b |b - \hat{b}_{m,i}(t+1)|^2 p_{b_i}(b) \mathcal{N}(b; \hat{q}_{m,i}(t), \nu_{m,i}^q(t)) \\ &\quad \nu_{m,i}^q(t) g'_{b_i}(\hat{q}_{m,i}(t), \nu_{m,i}^q(t)) \end{aligned} \quad (60)$$

where  $K = \int_b p_{b_i}(b) \mathcal{N}(b; \hat{q}_{m,i}(t), \nu_{m,i}^q(t))$  and where  $g'_{b_i}$  denotes the derivative of  $g_{b_i}$  with respect to the first argument. As before, we define the  $m$ -invariant quantities

$$\begin{aligned} \nu_i^q(t) &\triangleq \left[ \sum_m \left( \nu_m^s(t)\hat{z}_m^{(i,*)}(t)^2 \right. \right. \\ &\quad \left. \left. - (\hat{s}_m^2(t) - \nu_m^s(t)) \sum_{j=1}^{N_c} \nu_j^c(t)z_m^{(i,j)2} \right) \right]^{-1} \end{aligned} \quad (61)$$

$$\begin{aligned} \hat{q}_i(t) &\triangleq \hat{b}_i(t) + \nu_i^q(t) \sum_m \left( (\hat{s}_m^2(t) - \nu_m^s(t)) \right. \\ &\quad \left. \times \sum_{j=1}^{N_c} \nu_j^c(t)z_m^{(i,j)}\hat{z}_m^{(*,j)}(t) + \hat{s}_m(t)\hat{z}_{\rightarrow m}^{(i,*)}(t) \right) \end{aligned} \quad (62)$$

and perform several Taylor series expansions, finally dropping terms that vanish in the LSL, to obtain

$$\begin{aligned} \hat{b}_{m,i}(t+1) &= \hat{b}_i(t+1) - \hat{s}_m(t)\hat{z}_m^{(i,*)}(t)\nu_i^b(t+1) \\ &+ O(1/M^{3/2}), \end{aligned} \quad (63)$$

$$\hat{b}_i(t+1) \triangleq g_{b_i}(\hat{q}_i(t), \nu_i^q(t)) \quad (64)$$

$$\nu_i^b(t+1) \triangleq \nu_i^q(t)g'_{b_i}(\hat{q}_i(t), \nu_i^q(t)). \quad (65)$$

#### F. Closing the loop

To complete the derivation of P-BiG-AMP, we use (53) and (63) to eliminate the dependence on  $m$  in the  $b_i$  and  $c_j$  estimates and on  $i$  and  $j$  in the  $z_m$  estimates. By plugging (53) and (63) into the expression (24) for  $\hat{p}_m(t)$  and dropping terms that vanish in the LSL, it can be shown [10] that

$$\begin{aligned} \hat{p}_m(t) &\approx \hat{z}_m^{(*,*)}(t) - \hat{s}_m(t-1) \left( \sum_{i=1}^{N_b} \hat{z}_m^{(i,*)}(t-1)\hat{z}_m^{(i,*)}(t)\nu_i^b(t) \right. \\ &\quad \left. + \sum_{j=1}^{N_c} \hat{z}_m^{(*,j)}(t-1)\hat{z}_m^{(*,j)}(t)\nu_j^c(t) \right). \end{aligned} \quad (66)$$

Although not justified by the LSL, we also approximate

$$\sum_{i=1}^{N_b} \hat{z}_m^{(i,*)}(t-1)\hat{z}_m^{(i,*)}(t)\nu_i^b(t) \approx \sum_{i=1}^{N_b} \hat{z}_m^{(i,*)}(t)^2\nu_i^b(t) \quad (67)$$

$$\sum_{j=1}^{N_c} \hat{z}_m^{(*,j)}(t-1)\hat{z}_m^{(*,j)}(t)\nu_j^c(t) \approx \sum_{j=1}^{N_c} \hat{z}_m^{(*,j)}(t)^2\nu_j^c(t) \quad (68)$$

for the sake of algorithmic simplicity, yielding

$$\begin{aligned} \hat{p}_m(t) &\approx \hat{z}_m^{(*,*)}(t) - \hat{s}_m(t-1) \\ &\quad \times \underbrace{\left( \sum_{i=1}^{N_b} \hat{z}_m^{(i,*)}(t)^2\nu_i^b(t) + \sum_{j=1}^{N_c} \hat{z}_m^{(*,j)}(t)^2\nu_j^c(t) \right)}_{\triangleq \bar{\nu}_m^p(t)}, \end{aligned} \quad (69)$$

noting that similar approximations were made for BiG-AMP [20], where empirical tests showed little effect. Of course, a more complicated variant of P-BiG-AMP could be stated using (66) instead of (69).

Equations (53) and (63) can also be used to simplify  $\nu_m^p(t)$ . For this, we first use the facts  $\nu_{m,j}^c(t) = \nu_j^c(t) + O(1/M^{3/2})$  and  $\nu_{m,i}^b(t) = \nu_i^b(t) + O(1/M^{3/2})$  to write (25) as

$$\begin{aligned} \nu_m^p(t) &= \sum_{j=1}^{N_c} \nu_j^c(t)\hat{z}_{\rightarrow m}^{(*,j)}(t)^2 + \sum_{i=1}^{N_b} \nu_i^b(t)\hat{z}_{\rightarrow m}^{(i,*)}(t)^2 \\ &+ \sum_{i=1}^{N_b} \sum_{j=1}^{N_c} \nu_i^b(t)\nu_j^c(t)z_m^{(i,j)2} + O(1/M^{1/2}). \end{aligned} \quad (70)$$

Then we use (53) with (17) and (28) to write

$$\begin{aligned} \hat{z}_{\rightarrow m}^{(i,*)}(t) &= \hat{z}_m^{(i,*)}(t) - \hat{s}_m(t-1) \sum_{j=1}^{N_c} \hat{z}_m^{(*,j)}(t-1)z_m^{(i,j)}\nu_j^c(t) \\ &+ O(1/M), \end{aligned} \quad (71)$$

and similarly we use (63) to write

$$\begin{aligned} \hat{z}_{\rightarrow m}^{(*,j)}(t) &= \hat{z}_m^{(*,j)}(t) - \hat{s}_m(t-1) \sum_{i=1}^{N_b} \hat{z}_m^{(i,*)}(t-1)z_m^{(i,j)}\nu_i^b(t) \\ &+ O(1/M). \end{aligned} \quad (72)$$

Plugging (71)-(72) into (70) and dropping the terms that vanish in the LSL yields [10]

$$\nu_m^p(t) \approx \bar{\nu}_m^p(t) + \sum_{i=1}^{N_b} \sum_{j=1}^{N_c} \nu_i^b(t)\nu_j^c(t)z_m^{(i,j)2}. \quad (73)$$

Next, we eliminate the dependence on  $\hat{z}_{m,j}^{(*,j)}(t)$  from  $\hat{r}_j(t)$ . Plugging (72) into (49) and dropping the terms that vanish in the LSL yields

$$\begin{aligned} \hat{r}_j(t) &\approx \hat{c}_j(t) + \nu_j^r(t) \sum_m (\hat{s}_m^2(t) - \nu_m^s(t)) \\ &\quad \times \sum_{i=1}^{N_b} \nu_i^b(t) z_m^{(i,j)} \hat{z}_m^{(i,*)}(t) + \nu_j^r(t) \sum_m \hat{s}_m(t) \\ &\quad \times \left( \hat{z}_m^{(*,j)}(t) - \hat{s}_m(t-1) \sum_{i=1}^{N_b} \hat{z}_m^{(i,*)}(t-1) z_m^{(i,j)} \nu_i^b(t) \right), \end{aligned} \quad (74)$$

Although not justified by the LSL, we also approximate

$$\begin{aligned} \sum_m \hat{s}_m(t) \hat{s}_m(t-1) \sum_{i=1}^{N_b} \nu_i^b(t) z_m^{(i,j)} \hat{z}_m^{(i,*)}(t-1) \\ \approx \sum_m \hat{s}_m^2(t) \sum_{i=1}^{N_b} \nu_i^b(t) z_m^{(i,j)} \hat{z}_m^{(i,*)}(t) \end{aligned} \quad (75)$$

for the sake of algorithmic simplicity, yielding

$$\begin{aligned} \hat{r}_j(t) &\approx \hat{c}_j(t) + \nu_j^r(t) \sum_m \left( \hat{s}_m(t) \hat{z}_m^{(*,j)}(t) \right. \\ &\quad \left. - \nu_m^s(t) \sum_{i=1}^{N_b} \nu_i^b(t) z_m^{(i,j)} \hat{z}_m^{(i,*)}(t) \right), \end{aligned} \quad (76)$$

noting that a similar approximation was made for BiG-AMP [20]. The expression (76) then simplifies. Using (28) to expand  $\hat{z}_m^{(i,*)}(t)$ , the last term in (76) can be written as

$$\begin{aligned} \nu_j^r(t) \sum_m \nu_m^s(t) \sum_{i=1}^{N_b} \nu_i^b(t) z_m^{(i,j)} \hat{z}_m^{(i,*)}(t) \\ = \nu_j^r(t) \hat{c}_j(t) \sum_{i=1}^{N_b} \nu_i^b(t) \sum_m \nu_m^s(t) z_m^{(i,j)2} \end{aligned} \quad (77)$$

$$\begin{aligned} + \nu_j^r(t) \sum_{i=1}^{N_b} \nu_i^b(t) \sum_{k \neq j} \hat{c}_k(t) \sum_m \nu_m^s(t) z_m^{(i,j)} z_m^{(i,k)} \\ \approx \nu_j^r(t) \hat{c}_j(t) \sum_{i=1}^{N_b} \nu_i^b(t) \sum_m \nu_m^s(t) z_m^{(i,j)2}, \end{aligned} \quad (78)$$

where (78) holds in the LSL [10]. Thus, (76) reduces to

$$\begin{aligned} \hat{r}_j(t) &\approx \hat{c}_j(t) + \nu_j^r(t) \sum_m \hat{s}_m(t) \hat{z}_m^{(*,j)}(t) \\ &\quad - \nu_j^r(t) \hat{c}_j(t) \sum_m \nu_m^s(t) \sum_{i=1}^{N_b} \nu_i^b(t) z_m^{(i,j)2}. \end{aligned} \quad (79)$$

Similarly, we substitute (71) into (62) and make analogous approximations to obtain

$$\begin{aligned} \hat{q}_i(t) &\approx \hat{b}_i(t) + \nu_i^q(t) \sum_m \hat{s}_m(t) \hat{z}_m^{(*,*)}(t) \\ &\quad - \nu_i^q(t) \hat{b}_i(t) \sum_m \nu_m^s(t) \sum_{j=1}^{N_c} \nu_j^c(t) z_m^{(i,j)2}. \end{aligned} \quad (80)$$

Next, we simplify expressions for the variances  $\nu_j^r(t)$  and  $\nu_i^q(t)$ . First, it can be shown [10] that (38) and (39) can be used to rewrite the second half of  $\nu_j^r(t)$  from (48) as

$$\begin{aligned} \sum_m (\hat{s}_m^2(t) - \nu_m^s(t)) \sum_{i=1}^{N_b} \nu_i^b(t) z_m^{(i,j)2} \\ = \sum_m \left( \mathbb{E} \left\{ \frac{(z_m - \hat{p}_m(t))^2}{\nu_m^p(t)} \right\} - 1 \right) \frac{\sum_{i=1}^{N_b} \nu_i^b(t) z_m^{(i,j)2}}{\nu_m^p(t)}, \end{aligned} \quad (81)$$

where the random variable  $\mathbf{z}_m$  above is distributed according to the pdf in line (D1) of Table II. For the G-AMP algorithm, [19, Sec. VI.D] clarifies that, under i.i.d priors and scalar variances, in the LSL, the true  $\mathbf{z}_m$  and the G-AMP iterates  $\hat{\mathbf{p}}_m(t)$  converge empirically to a pair of random variables  $(\mathbf{z}, \mathbf{p})$  that satisfy  $p_{z|\mathbf{p}}(z|\hat{\mathbf{p}}(t)) = \mathcal{N}(z; \hat{\mathbf{p}}(t), \nu^p(t))$ . This suggests that (81) is negligible in the LSL, in which case (48) implies

$$\nu_j^r(t) \approx \left( \sum_m \nu_m^s(t) \hat{z}_m^{(*,j)}(t)^2 \right)^{-1}. \quad (82)$$

A similar argument yields

$$\nu_i^q(t) \approx \left( \sum_m \nu_m^s(t) \hat{z}_m^{(i,*)}(t)^2 \right)^{-1}. \quad (83)$$

The final step in the derivation of P-BiG-AMP is to approximate the SPA posterior log-pdfs in (14) and (15). Plugging (35) and (42) into these expressions, we get

$$\Delta_i^b(t+1, b_i) \approx \text{const} + \log(p_{b_i|y}(b_i; \hat{q}_i(t), \nu_i^q(t))) \quad (84)$$

$$\Delta_j^c(t+1, c_j) \approx \text{const} + \log(p_{c_j|y}(c_j; \hat{r}_j(t), \nu_j^r(t))) \quad (85)$$

using steps similar to those used for (43). The corresponding pdfs are given as (D2) and (D3) in Table II and represent P-BiG-AMP's iteration- $t$  approximations to the true marginal posteriors  $p_{b_i|y}(b_i | \mathbf{y})$  and  $p_{c_j|y}(c_j | \mathbf{y})$ . The quantities  $\hat{b}_i(t+1)$  and  $\nu_i^b(t+1)$  are then respectively defined as the mean and variance of the pdf associated with (84), and  $\hat{c}_j(t+1)$  and  $\nu_j^c(t+1)$  are the mean and variance of the pdf associated with (85). This completes the derivation of P-BiG-AMP.

A table summarizing the steps of the P-BiG-AMP algorithm is given in [10] but is omitted here for reasons of space.

### G. Scalar-Variance Approximation

The P-BiG-AMP algorithm derived above stores and processes variance terms  $\bar{\nu}_m^p, \nu_m^p, \nu_m^s, \nu_m^r, \nu_j^q, \nu_j^r, \nu_i^q, \nu_i^b$  that depend on the indices  $m, j, i$ . The use of scalar (i.e., index-invariant) variances significantly reduces its complexity.

To derive scalar-variance P-BiG-AMP, we first assume  $\forall i : \nu_i^b(t) \approx \nu^b(t) \triangleq \frac{1}{N_b} \sum_{i=1}^{N_b} \nu_i^b(t)$  and  $\forall j : \nu_j^c(t) \approx \nu^c(t) \triangleq \frac{1}{N_c} \sum_{j=1}^{N_c} \nu_j^c(t)$ . Then we approximate  $\bar{\nu}_m^p(t)$  as

$$\bar{\nu}_m^p(t) \approx \nu^b(t) \sum_{i=1}^{N_b} |\hat{z}_m^{(i,*)}(t)|^2 + \nu^c(t) \sum_{j=1}^{N_c} |\hat{z}_m^{(*,j)}(t)|^2 \quad (86)$$

$$\approx \frac{\nu^b(t)}{M} \sum_{i=1}^{N_b} \|\hat{\mathbf{z}}^{(i,*)}(t)\|^2 + \frac{\nu^c(t)}{M} \sum_{j=1}^{N_c} \|\hat{\mathbf{z}}^{(*,j)}(t)\|^2 \triangleq \bar{\nu}^p(t). \quad (87)$$

Similarly,  $\nu_m^p(t)$  is approximated as

$$\nu_m^p(t) \approx \bar{\nu}^p(t) + \nu^b(t) \nu^c(t) \sum_{i=1}^{N_b} \sum_{j=1}^{N_c} |z_m^{(i,j)}|^2 \quad (88)$$

$$\approx \bar{\nu}^p(t) + \frac{\nu^b(t) \nu^c(t)}{M} \sum_{i=1}^{N_b} \sum_{j=1}^{N_c} \|\mathbf{z}^{(i,j)}\|^2 \triangleq \nu^p(t), \quad (89)$$

where  $\frac{1}{M} \sum_{i=1}^{N_b} \sum_{j=1}^{N_c} \|\mathbf{z}^{(i,j)}\|^2$  can be pre-computed. Even with the above scalar-variance approximations,  $\nu_m^s(t)$  is not guaranteed to be  $m$ -invariant. Still, it can be approximated as such using  $\nu^s(t) \triangleq \frac{1}{M} \sum_{m=1}^M \nu_m^s(t)$ , in which case

$$\nu_j^r(t) \approx (\nu^s(t) \|\hat{\mathbf{z}}^{(*,j)}(t)\|^2)^{-1} \quad (90)$$

$$\approx (\nu^s(t) \frac{1}{N_c} \sum_{j=1}^{N_c} \|\hat{\mathbf{z}}^{(*,j)}(t)\|^2)^{-1} \triangleq \nu^r(t) \quad (91)$$

$$\begin{aligned} \hat{r}_j(t) &= \hat{c}_j(t) + \nu^r(t) \sum_{m=1}^M \hat{s}_m(t) \hat{z}_m^{(*,j)}(t)^* \\ &\quad - \nu^r(t) \nu^s(t) \nu^b(t) \hat{c}_j(t) \sum_{i=1}^{N_b} \|\mathbf{z}^{(i,j)}\|^2, \end{aligned} \quad (92)$$

where  $\sum_{i=1}^{N_b} \|\mathbf{z}^{(i,j)}\|^2$  can be pre-computed. Similarly,

$$\nu_i^q(t) \approx (\nu^s(t) \|\hat{\mathbf{z}}^{(i,*)}(t)\|^2)^{-1} \quad (93)$$

$$\approx (\nu^s(t) \frac{1}{N_b} \sum_{i=1}^{N_b} \|\hat{\mathbf{z}}^{(i,*)}(t)\|^2)^{-1} \triangleq \nu^q(t) \quad (94)$$

$$\begin{aligned} \hat{q}_i(t) &= \hat{b}_i(t) + \nu^q(t) \sum_{m=1}^M \hat{s}_m(t) \hat{z}_m^{(i,*)}(t)^* \\ &\quad - \nu^q(t) \nu^s(t) \nu^c(t) \hat{b}_i(t) \sum_{j=1}^{N_c} \|\mathbf{z}^{(i,j)}\|^2. \end{aligned} \quad (95)$$

The scalar-variance P-BiG-AMP algorithm is summarized in Table II. Noting the Hermitian transposes in lines (R12)

definitions:	
$p_{z_m   p_m}(z   \hat{p}; \nu^p) \triangleq \frac{p_{y_m   z_m}(y_m   z) \mathcal{N}(z; \hat{p}, \nu^p)}{\int_{z'} p_{y_m   z_m}(y_m   z') \mathcal{N}(z'; \hat{p}, \nu^p)}$	(D1)
$p_{c_j   r_j}(c   \hat{r}; \nu^r) \triangleq \frac{p_{c_j}(c) \mathcal{N}(c; \hat{r}, \nu^r)}{\int_{c'} p_{c_j}(c') \mathcal{N}(c'; \hat{r}, \nu^r)}$	(D2)
$p_{b_i   q_i}(b   \hat{q}; \nu^q) \triangleq \frac{p_{b_i}(b) \mathcal{N}(b; \hat{q}, \nu^q)}{\int_{b'} p_{b_i}(b') \mathcal{N}(b'; \hat{q}, \nu^q)}$	(D3)
initialization:	
$\forall m : \hat{s}_m(0) = 0$	(I1)
$\forall i, j : \text{choose } \hat{b}_i(1), \nu^b(1), \hat{c}_j(1), \nu^c(1)$	(I2)
for $t = 1, \dots, T_{\max}$	
$\forall i : \hat{z}^{(i,*)}(t) = \sum_{j=0}^{N_c} \hat{z}^{(i,j)} \hat{c}_j(t)$	(R1)
$\forall j : \hat{z}^{(*,j)}(t) = \sum_{i=0}^{N_b} \hat{b}_i(t) \hat{z}^{(i,j)}$	(R2)
$\hat{z}^{(*,*)}(t) = \sum_{i=0}^{N_b} \hat{b}_i(t) \hat{z}^{(i,*)}(t) \text{ or } \sum_{j=0}^{N_c} \hat{c}_j(t) \hat{z}^{(*,j)}(t)$	(R3)
$\bar{\nu}^p(t) = (\nu^b(t) \sum_{i=1}^{N_b} \ \hat{z}^{(i,*)}(t)\ ^2 + \nu^c(t) \sum_{j=1}^{N_c} \ \hat{z}^{(*,j)}(t)\ ^2) / M$	(R4)
$\nu^p(t) = \bar{\nu}^p(t) + \nu^b(t) \nu^c(t) \sum_{i=1}^{N_b} \sum_{j=1}^{N_c} \ \hat{z}^{(i,j)}\ ^2 / M$	(R5)
$\hat{p}(t) = \hat{z}^{(*,*)}(t) - \hat{s}(t-1) \bar{\nu}^p(t)$	(R6)
$\nu^z(t) = \sum_{m=1}^M \text{var}\{z_m   p_m = \hat{p}_m(t); \nu^p(t)\} / M$	(R7)
$\forall m : \hat{z}_m(t) = E\{z_m   p_m = \hat{p}_m(t); \nu^p(t)\}$	(R8)
$\nu^s(t) = (1 - \nu^z(t) / \nu^p(t)) / \nu^p(t)$	(R9)
$\hat{s}(t) = (\hat{z}(t) - \hat{p}(t)) / \nu^p(t)$	(R10)
$\nu^r(t) = (\nu^s(t) \sum_{j=1}^{N_c} \ \hat{z}^{(*,j)}(t)\ ^2 / N_c)^{-1}$	(R11)
$\forall j : \hat{r}_j(t) = (1 - \nu^r(t) \nu^s(t) \nu^b(t) \sum_{i=1}^{N_b} \ \hat{z}^{(i,j)}\ ^2) \hat{c}_j(t) + \nu^r(t) \hat{z}^{(*,j)H}(t) \hat{s}(t)$	(R12)
$\nu^q(t) = (\nu^s(t) \sum_{i=1}^{N_b} \ \hat{z}^{(i,*)}(t)\ ^2 / N_b)^{-1}$	(R13)
$\forall i : \hat{q}_i(t) = (1 - \nu^q(t) \nu^s(t) \nu^c(t) \sum_{j=1}^{N_c} \ \hat{z}^{(i,j)}\ ^2) \hat{b}_i(t) + \nu^q(t) \hat{z}^{(i,*)H}(t) \hat{s}(t)$	(R14)
$\nu^c(t+1) = \sum_{j=1}^{N_c} \text{var}\{c_j   r_j = \hat{r}_j(t); \nu_j^r(t)\} / N_c$	(R15)
$\forall j : \hat{c}_j(t+1) = E\{c_j   r_j = \hat{r}_j(t); \nu_j^r(t)\}$	(R16)
$\nu^b(t+1) = \sum_{i=1}^{N_b} \text{var}\{b_i   q_i = \hat{q}_i(t); \nu_i^q(t)\} / N_b$	(R17)
$\forall i : \hat{b}_i(t+1) = E\{b_i   q_i = \hat{q}_i(t); \nu_i^q(t)\}$	(R18)
if $\ \hat{z}^{(*,*)}(t) - \hat{z}^{(*,*)}(t-1)\ ^2 \leq \tau_{\text{stop}} \ \hat{z}^{(*,*)}(t)\ ^2$ , stop	(R19)
end	

TABLE II  
THE SCALAR-VARIANCE P-BiG-AMP ALGORITHM

(R1)	$O(MN_bN_c)$	(R2)	$O(MN_bN_c)$	(R3)	$O(M(N_b \wedge N_c))$
(R4)	$O(1)$	(R5)	$O(1)$	(R6)	$O(M)$
(R7)	$O(M)$	(R8)	$O(M)$	(R9)	$O(M)$
(R10)	$O(M)$	(R11)	$O(1)$	(R12)	$O(MN_c)$
(R13)	$O(1)$	(R14)	$O(MN_b)$	(R15)	$O(N_c)$
(R16)	$O(N_c)$	(R17)	$O(N_b)$	(R18)	$O(N_b)$

TABLE III  
WORST-CASE COMPLEXITY OF SCALAR-VARIANCE P-BiG-AMP.

and (R14), the algorithm allows the use of complex-valued quantities, in which case  $\mathcal{N}$  in (D1)-(D3) becomes a circular complex Gaussian pdf. The complexity scaling of each line in Table II is tabulated in Table III assuming that all  $MN_bN_c$  entries in the tensor  $z_m^{(i,j)}$  are nonzero. In practice,  $z_m^{(i,j)}$  is often sparse or implementable using a fast transformation, allowing drastic reduction in complexity, as shown in Section IV. Thus, Table III should be interpreted as “worst-case” complexity.

#### H. Damping

Damping has been applied to both G-AMP [46] and BiG-AMP [20] to prevent divergence. Essentially, damping (or “relaxation” in the optimization literature) slows the evolution of the algorithm’s state variables. For G-AMP, damping yields provable local-convergence guarantees with arbitrary matri-

ces [46] while, for BiG-AMP, damping has been shown to be very effective through an extensive empirical study [21]. Furthermore, *adaptive* damping has been proposed for G-AMP with the goal of preventing divergence with minimal impact on runtime [47]. The same damping strategies can be straightforwardly applied to P-BiG-AMP. For details, we direct the interested reader to [10] and the public domain GAMPmatlab implementation [48].

#### I. Tuning of the Prior and Likelihood

To run P-BiG-AMP, one must specify the priors and likelihood in lines (D1)-(D3) of Table II. Although a reasonable family of distributions may be dictated by the application, the specific parameters of the distributions must often be tuned in practice. To address this issue, we propose to apply the expectation-maximization (EM) [23] based approach developed for G-AMP [25] and later extended to BiG-AMP in [20]. In this approach, the user specifies the families of P-BiG-AMP priors  $\{p_{b_i}(\cdot; \theta), p_{c_j}(\cdot; \theta), p_{y_m | z_m}(y_m | \cdot; \theta)\}_{\forall m,n,l}$  and the EM algorithm is used to (locally) maximize the likelihood of the parameter vector  $\theta$ , i.e., to find  $\hat{\theta} \triangleq \arg \max_{\theta} p_Y(y; \theta)$ . If the families themselves are unknown, it may suffice to use Gaussian-mixture models and learn their parameters [25]. Since the details are nearly identical to the BiG-AMP case, we omit them and refer the reader to [10].

### IV. EXAMPLE PARAMETERIZATIONS

P-BiG-AMP was summarized and derived in Section III for generic parameterizations  $z^{(i,j)}$  in (4). A naive implementation, which treats every  $z_m^{(i,j)}$  as nonzero, would lead to the worst-case complexities stated in Table III. In practice, however,  $\{z_m^{(i,j)}\}$  is often sparse or implementable using a fast transformation, in which case the implementation can be dramatically simplified. We now describe several examples of structured  $z^{(i,j)}$ , detailing the computations needed for the essential scalar-variance P-BiG-AMP quantities  $\hat{z}^{(*,*)}(t)$ ,  $\sum_{i=1}^{N_b} \|\hat{z}^{(i,*)}(t)\|^2$ ,  $\sum_{j=1}^{N_c} \|\hat{z}^{(*,j)}(t)\|^2$ ,  $\{\hat{z}^{(i,*)H}(t) \hat{s}(t)\}_{i=1}^{N_b}$  and  $\{\hat{z}^{(*,j)H}(t) \hat{s}(t)\}_{j=1}^{N_c}$ .

#### A. Multi-snapshot Structure

With multi-snapshot structure, the noiseless outputs become

$$\mathbf{Z} = \sum_{i=0}^{N_b} b_i \mathbf{A}^{(i)} \mathbf{C} \text{ with known } \{\mathbf{A}^{(i)}\}, \quad (96)$$

where  $\mathbf{Z} \in \mathbb{C}^{K \times L}$  and  $\mathbf{C} \in \mathbb{C}^{N \times L}$  for<sup>6</sup>  $L > 1$ . Thus we have  $\mathbf{A}^{(i)} \in \mathbb{C}^{K \times N}$ ,  $M = KL$ , and  $N_c = NL$ . Defining  $\mathbf{z} \triangleq \text{vec}(\mathbf{Z})$  and  $\mathbf{c} \triangleq \text{vec}(\mathbf{C})$ , we find

$$\mathbf{z} = \sum_{i=0}^{N_b} b_i (\mathbf{I}_L \otimes \mathbf{A}^{(i)}) \mathbf{c}, \quad (97)$$

<sup>6</sup>When  $L = 1$ , (96) reduces to the general parameterization (4).



which implies that

$$\mathbf{z}^{(i,j)} = [\mathbf{I}_L \otimes \mathbf{A}^{(i)}]_{:,j} \quad (98)$$

$$\hat{\mathbf{z}}^{(i,*)}(t) = \text{vec}(\mathbf{A}^{(i)} \hat{\mathbf{C}}(t)) \quad (99)$$

$$\hat{\mathbf{z}}^{(*,j)}(t) = [\mathbf{I}_L \otimes \hat{\mathbf{A}}(t)]_{:,j} \quad (100)$$

$$\hat{\mathbf{z}}^{(*,*)}(t) = \sum_{i=1}^{N_b} \hat{b}_i(t) \text{vec}(\mathbf{A}^{(i)} \hat{\mathbf{C}}(t)) = \text{vec}(\hat{\mathbf{A}}(t) \hat{\mathbf{C}}(t)) \quad (101)$$

$$\hat{\mathbf{A}}(t) \triangleq \sum_{i=1}^{N_b} \hat{b}_i(t) \mathbf{A}^{(i)}, \quad (102)$$

where  $[\mathbf{X}]_{:,j}$  denotes the  $j$ th column of  $\mathbf{X}$  and  $\hat{\mathbf{C}}(t) \in \mathbb{C}^{N \times L}$  is a reshaping of  $\hat{\mathbf{c}}(t)$ . Note that (98)-(100) follow directly from (97) via the derivative interpretations (32)-(34).

From the above expressions, it can be readily shown that

$$\sum_{i=1}^{N_b} \|\hat{\mathbf{z}}^{(i,*)}(t)\|^2 = \sum_{i=1}^{N_b} \|\mathbf{A}^{(i)} \hat{\mathbf{C}}(t)\|_F^2 = \text{tr}(\mathbf{\Gamma} \hat{\mathbf{C}}(t) \hat{\mathbf{C}}(t)^H) \quad (103)$$

$$\sum_{j=1}^{N_c} \|\hat{\mathbf{z}}^{(*,j)}(t)\|^2 = L \|\hat{\mathbf{A}}(t)\|_F^2 \quad (104)$$

with pre-computed

$$\mathbf{\Gamma} \triangleq \sum_{i=1}^{N_b} \mathbf{A}^{(i)H} \mathbf{A}^{(i)}. \quad (105)$$

Furthermore, under the scalar variance approximation,

$$\begin{aligned} \hat{\mathbf{R}}(t) &= (1 - \nu^r(t) \nu^s(t) \nu^b(t) D^r) \hat{\mathbf{C}}(t) \\ &\quad + \nu^r(t) \hat{\mathbf{A}}^H(t) \hat{\mathbf{S}}(t) \end{aligned} \quad (106)$$

$$\begin{aligned} \hat{\mathbf{Q}}(t) &= (1 - \nu^q(t) \nu^s(t) \nu^c(t) D^q) \hat{\mathbf{b}}(t) \\ &\quad + \nu^q(t) \begin{bmatrix} \text{vec}(\mathbf{A}^{(1)} \hat{\mathbf{C}}(t))^H \\ \vdots \\ \text{vec}(\mathbf{A}^{(N_b)} \hat{\mathbf{C}}(t))^H \end{bmatrix} \hat{\mathbf{s}}(t), \end{aligned} \quad (107)$$

with the following pre-computed using  $\mathbf{a}_n^{(i)} \triangleq [\mathbf{A}^{(i)}]_{:,n}$ :

$$D^r \triangleq \text{diag} \{ \sum_{i=1}^{N_b} \|\mathbf{a}_1^{(i)}\|^2, \dots, \sum_{i=1}^{N_b} \|\mathbf{a}_N^{(i)}\|^2 \} \quad (108)$$

$$D^q \triangleq L \text{diag} \{ \|\mathbf{A}^{(1)}\|_F^2, \dots, \|\mathbf{A}^{(N_b)}\|_F^2 \} \quad (109)$$

Note that (101)-(109) specify the essential quantities needed for the implementation of scalar-variance P-BiG-AMP. We discuss the complexity of these steps for two cases below.

First, suppose w.l.o.g. that each  $\mathbf{A}^{(i)}$  has  $N_a \leq KN$  nonzero elements, with possibly different supports among  $\{\mathbf{A}^{(i)}\}$ . This implies that  $\hat{\mathbf{A}}(t)$  has at most  $\min(N_b N_a, KN)$  nonzero elements. It then follows that (101) consumes  $\min(N_b N_a, KN)L$  multiplies, (102) consumes  $N_b N_a$ , (103) consumes  $L \min(N_b(N_a + K), N^2)$  and (104) consumes  $\min(N_b N_a, KN)$  multiplies. Furthermore, (106) consumes  $\approx \min(N_b N_a, KN)L$  multiplies and (107) consumes  $\approx N_b L(N_a + K)$ . In total,  $O(\min(N_b N_a, KN)L + N_b N_a L + N_b K L + L \min(N_b(N_a + K), N^2))$  multiplies are consumed. For illustration, suppose that  $N_b N_a < KN$  and  $N_b N_a < N^2$ . Then  $O(NL + N_b L(N_a + K))$  multiplies are consumed, in contrast to  $O(MN_b N_c) = O(KNL^2 N_b)$  for the general case.

Now suppose w.l.o.g. that, for a given  $\mathbf{b}$ , the multiplication of  $\mathbf{A}(\mathbf{b})$  by a vector  $\mathbf{x}$  can be accomplished implicitly using  $N_a$  multiplies. For example,  $N_a = O(N \log N)$  in the case of an FFT. Then (101) consumes  $N_a L$  multiplies, (103) consumes  $KL$  (using  $\{\mathbf{A}^{(i)} \hat{\mathbf{C}}(t)\}$  computed for  $\hat{\mathbf{Q}}(t)$ ), and (104) can

be approximated using  $O(N_a)$  multiplies. Furthermore, (106) consumes  $\approx (N + N_a)L$  multiplies and (107) consumes  $\approx N_b L(N_a + K)$ . In total,  $O(L(N + N_b N_a + N_b K))$  multiplies are consumed, in contrast to  $O(MN_b N_c) = O(KNL^2 N_b)$  for the general case.

### B. Low-Rank Structure

With low-rank signal structure, the noiseless outputs become

$$z_m = \text{tr}(\Phi_m^H \mathbf{B}^T \mathbf{C}), \quad m = 1, \dots, M, \quad (110)$$

with known  $\{\Phi_m\}$ , where  $\mathbf{B} \in \mathbb{C}^{N \times K}$ ,  $\mathbf{C} \in \mathbb{C}^{N \times L}$  for  $N > 1$ . Thus we have  $\Phi_m \in \mathbb{C}^{K \times L}$ ,  $N_b = NK$ , and  $N_c = NL$ . Defining  $\phi_m \triangleq \text{vec}(\Phi_m)$ ,  $\mathbf{b} \triangleq \text{vec}(\mathbf{B})$ , and  $\mathbf{c} \triangleq \text{vec}(\mathbf{C})$ ,

$$z_m = \phi_m^H \text{vec}(\mathbf{B}^T \mathbf{C}) = \mathbf{b}^T (\Phi_m^* \otimes \mathbf{I}_N) \mathbf{c} \quad (111)$$

$$= \text{vec}(\mathbf{B} \Phi_m^*)^T \mathbf{c} \quad (112)$$

$$= \text{vec}(\mathbf{C} \Phi_m^H) \mathbf{b} \quad (113)$$

from which the derivative interpretations (32)-(34) imply

$$\mathbf{z}^{(i,j)} = \begin{bmatrix} [\Phi_1 \otimes \mathbf{I}_N]_{i,j} \\ \vdots \\ [\Phi_M \otimes \mathbf{I}_N]_{i,j} \end{bmatrix}, \quad \hat{\mathbf{z}}^{(*,*)}(t) = \begin{bmatrix} \text{tr}(\Phi_1^H \hat{\mathbf{B}}(t)^T \hat{\mathbf{C}}(t)) \\ \vdots \\ \text{tr}(\Phi_M^H \hat{\mathbf{B}}(t)^T \hat{\mathbf{C}}(t)) \end{bmatrix} \quad (114)$$

$$\hat{\mathbf{z}}^{(i,*)}(t) = \begin{bmatrix} \text{vec}(\hat{\mathbf{C}}(t) \Phi_1^H)^T \\ \vdots \\ \text{vec}(\hat{\mathbf{C}}(t) \Phi_M^H)^T \end{bmatrix}_{:,i}, \quad \hat{\mathbf{z}}^{(*,j)}(t) = \begin{bmatrix} \text{vec}(\hat{\mathbf{B}}(t) \Phi_1^*)^T \\ \vdots \\ \text{vec}(\hat{\mathbf{B}}(t) \Phi_M^*)^T \end{bmatrix}_{:,j}. \quad (115)$$

From the above expressions, it can be readily shown that

$$\sum_{i=1}^{N_b} \|\hat{\mathbf{z}}^{(i,*)}(t)\|^2 = \sum_{m=1}^M \|\Phi_m \hat{\mathbf{C}}(t)^H\|_F^2 \quad (116a)$$

$$= \text{tr}(\mathbf{\Gamma}_1 \hat{\mathbf{C}}(t)^H \hat{\mathbf{C}}(t)) \quad (116b)$$

$$\sum_{j=1}^{N_c} \|\hat{\mathbf{z}}^{(*,j)}(t)\|^2 = \sum_{m=1}^M \|\hat{\mathbf{B}}(t)^* \Phi_m\|_F^2 \quad (117a)$$

$$= \text{tr}(\mathbf{\Gamma}_2 \hat{\mathbf{B}}(t)^T \hat{\mathbf{B}}(t)^*) \quad (117b)$$

with pre-computed

$$\mathbf{\Gamma}_1 \triangleq \sum_{m=1}^M \Phi_m^H \Phi_m, \quad \mathbf{\Gamma}_2 \triangleq \sum_{m=1}^M \Phi_m \Phi_m^H. \quad (118)$$

Furthermore, under the scalar variance approximation,

$$\begin{aligned} \hat{\mathbf{R}}(t) &= \hat{\mathbf{C}}(t) (\mathbf{I}_L - \nu^r(t) \nu^s(t) \nu^b(t) \text{Diag} \mathbf{\Gamma}_1) \\ &\quad + \nu^r(t) \hat{\mathbf{B}}(t)^* \left( \sum_{m=1}^M \hat{s}_m(t) \Phi_m \right) \end{aligned} \quad (119)$$

$$\begin{aligned} \hat{\mathbf{Q}}(t) &= \hat{\mathbf{B}}(t) (\mathbf{I}_K - \nu^q(t) \nu^s(t) \nu^c(t) \text{Diag} \mathbf{\Gamma}_2) \\ &\quad + \nu^q(t) \hat{\mathbf{C}}(t)^* \left( \sum_{m=1}^M \hat{s}_m(t) \Phi_m^T \right). \end{aligned} \quad (120)$$

Note that (114)-(120) specify the essential quantities needed for the implementation of scalar-variance P-BiG-AMP. We discuss the complexity of these steps below.

Suppose w.l.o.g. that  $\Phi_m$  has  $N_\phi \leq KL$  nonzero entries, with possibly different supports among  $\{\Phi_m\}$ . This implies that  $\sum_m \hat{s}_m(t) \Phi_m$  has at most  $\min(KL, MN_\phi)$  nonzero elements. It then follows that  $\hat{\mathbf{z}}^{(*,*)}(t)$  from

<sup>7</sup>When  $N = 1$ , (110) reduces to the general parameterization (4).

(114) consumes  $NKL + MN_\phi$  multiplies, (116) consumes  $\approx N \min\{L^2, M(N_\phi + K)\}$ , and (117) consumes  $\approx N \min\{K^2, M(N_\phi + L)\}$ . Furthermore, (119) consumes  $NL + N \min(KL, MN_\phi) + MN_\phi$  multiplies and (120) consumes  $NK + N \min(KL, MN_\phi)$ . In total,  $O(N \min(L^2, M(N_\phi + K)) + N \min(K^2, M(N_\phi + L)) + NKL + MN_\phi)$  multiplies are consumed. For illustration, suppose that  $N_\phi < K, L$  and  $M < K, L$ . Then  $O(NKL)$  multiplies are consumed, in contrast to  $O(MN_bN_c) = O(MN^2KL)$  in the general case.

### C. Matrix-product Structure

A special case of (96) and (110) is when

$$\mathbf{Z} = \mathbf{BC} \quad (121)$$

which occurs, e.g., in applications such as MC, RPCA, DL, and NMF, as discussed in Section I-A. In particular, (96) reduces to (121) when  $N_b = KN$  and  $\text{vec}(\mathbf{A}^{(i)}) = [\mathbf{I}]_{:,i}$ , and (110) reduces to (121) when  $M = KL$  and  $\text{vec}(\mathbf{\Phi}_m) = [\mathbf{I}]_{:,m}$ . It can be verified [1] that, under (121), P-BiG-AMP reduces to BiG-AMP from [20].

### D. Low-Rank plus Sparse Structure

Recall (3), the problem of recovering a “low-rank plus sparse” matrix. Writing the low-rank component as  $\mathbf{L} = \mathbf{B}^\top \mathbf{C}_1$  with  $\mathbf{B} \in \mathbb{C}^{N \times K}$ ,  $\mathbf{C}_1 \in \mathbb{C}^{N \times L}$ , and  $N < \min\{K, L\}$ , we can invoke (111) to get

$$z_m = \mathbf{b}^\top (\mathbf{\Phi}_m^* \otimes \mathbf{I}_N) \mathbf{c}_1 + \phi_m^H \mathbf{c}_2, \quad m = 1, \dots, M, \quad (122)$$

with  $b_0 \triangleq 1$  (recall Section I-B),  $\mathbf{b} \triangleq \text{vec}(\mathbf{B})$ ,  $\mathbf{c}_1 \triangleq \text{vec}(\mathbf{C})$ ,  $\mathbf{c}_2 \triangleq \text{vec}(\mathbf{S})$  (recall  $\mathbf{S}$  was the sparse matrix from (3)), and  $\mathbf{c} = [\mathbf{c}_1^\top, \mathbf{c}_2^\top]^\top$ .

Note that the structure of the first term of (122) can be exploited through (114)-(115), as discussed in Section IV-B. Meanwhile, straightforward computational simplifications of the second term in (122) result when  $\phi_m^H$  is sparse. But care must be taken in applying the scalar-variance approximation in this case: it may be advantageous to use different scalar variances for  $\mathbf{c}_1$  and  $\mathbf{c}_2$  (e.g.,  $\nu_1^r, \nu_1^c$  and  $\nu_2^r, \nu_2^c$ ).

## V. NUMERICAL EXPERIMENTS

We now present the results of several numerical experiments that test the performance of P-BiG-AMP and EM-P-BiG-AMP in various applications. In most cases, we quantify recovery performance using  $\text{NMSE}(\hat{\mathbf{b}}) \triangleq \|\mathbf{b} - \hat{\mathbf{b}}\|_2^2 / \|\mathbf{b}\|_2^2$  and  $\text{NMSE}(\hat{\mathbf{c}}) \triangleq \|\mathbf{c} - \hat{\mathbf{c}}\|_2^2 / \|\mathbf{c}\|_2^2$ . Matlab code for P-BiG-AMP and EM-P-BiG-AMP can be found in [48].

### A. I.i.d. Gaussian Model

First, we examine the performance of P-BiG-AMP in the case of i.i.d. Gaussian  $z_m^{(i,j)}$ , as assumed for its derivation. In particular,  $\{z_m^{(i,j)}\}$  were drawn i.i.d.  $\mathcal{CN}(0, 1)$ ,  $\mathbf{b} = [b_1, \dots, b_{N_b}]^\top$  were drawn Bernoulli- $\mathcal{CN}(0, 1)$  with sparsity rate  $\xi^b$ , and  $\mathbf{c} = [c_1, \dots, c_{N_c}]^\top$  were drawn Bernoulli- $\mathcal{CN}(0, \nu^c)$  with sparsity rate  $\xi^c$ . We then attempted to recover  $\mathbf{b}$  and  $\mathbf{c}$  from  $M$  noiseless measurements of the form (4) under known  $b_0 = \sqrt{N_b}$  and  $c_0 = \sqrt{N_c}$ . For our experiment, we used

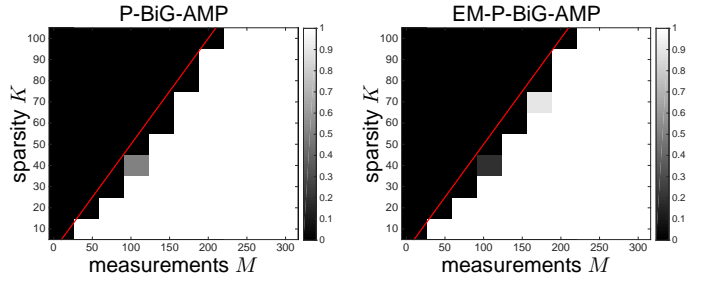


Fig. 2. Empirical success rate for noiseless sparse signal recovery under the i.i.d. parametric bilinear model (4) as a function of the number of measurements  $M$  and the signal sparsity  $K$ . Success rates were averaged over 10 problem realizations. Points above the red curve are infeasible due to counting bound, as described in the text.

$N_b = N_c = 100$  and  $\nu^c = 1$ , and we varied both the sparsity rate  $\xi^b = \xi^c = K/100$  and the number of measurements  $M$ .

We tested the performance of both P-BiG-AMP, which assumed oracle knowledge of all distributional parameters, and EM-P-BiG-AMP, which estimated the parameters  $\boldsymbol{\theta} \triangleq [\nu^c, \xi^b, \xi^c]^\top$  as well as the additive white Gaussian noise (AWGN) variance.<sup>8</sup> Figure 2 shows the empirical success rate for both algorithms, averaged over 10 independent problem realizations, as a function of the sparsity  $K$  and the number of measurements  $M$ . Here, we declare a “success” when both  $\text{NMSE}(\hat{\mathbf{b}}) < -60$  dB and  $\text{NMSE}(\hat{\mathbf{c}}) < -60$  dB. The figure shows that both P-BiG-AMP and EM-P-BiG-AMP gave sharp phase transitions. Moreover, their phase transitions are very close to the counting bound “ $M \geq 2K$ ,” shown by the red line in Fig. 2.

### B. Self Calibration

We now consider the self calibration problem described in Section I-A. In particular, we consider the noiseless single measurement vector (SMV) version, where the goal is to jointly recover the  $K$ -sparse signal  $\mathbf{c} \in \mathbb{R}^{N_c}$  and calibration parameters  $\mathbf{b} \in \mathbb{R}^{N_b}$  from  $M$  noiseless measurements of the form  $\mathbf{z} = \text{Diag}(\mathbf{H}\mathbf{b})\mathbf{A}\mathbf{c}$ , where  $\mathbf{H}$  and  $\mathbf{A}$  are known. For our experiment, we mimic the setup used for [8, Figure 1]. Thus, we set  $N_c = 256$  and  $M = 128$ , we chose  $\mathbf{H}$  as the first  $N_b$  columns of a  $M$ -point unitary DFT matrix, and we drew the entries of  $\mathbf{A}$  as i.i.d.  $\mathcal{N}(0, 1)$ . Furthermore, we drew  $K$ -sparse  $\mathbf{c}$  with i.i.d.  $\mathcal{N}(0, \nu^c)$  non-zero elements chosen uniformly at random, and we drew  $\mathbf{b}$  as i.i.d.  $\mathcal{N}(0, 1)$ .

We compared the performance of EM-P-BiG-AMP to SparseLift [8], a recently proposed convex relaxation, using CVX for the implementation. EM-P-BiG-AMP modeled  $\mathbf{c}$  as Bernoulli- $\mathcal{N}(0, \nu^c)$  and learned  $\nu^c$ , the sparsity rate  $\xi$ , and the AWGN variance.<sup>9</sup> Figure 3 shows empirical success rate as a function of signal sparsity  $K$  and number of calibration parameters  $N_b$ . As in [8], we considered  $\text{NMSE} \triangleq \|\mathbf{b}\mathbf{c}^\top - \hat{\mathbf{b}}\hat{\mathbf{c}}^\top\|_F^2 / \|\mathbf{b}\mathbf{c}^\top\|_F^2$ , and we declared “success” when  $\text{NMSE} < -60$  dB. Figure 3 shows that EM-P-BiG-AMP’s success region was much larger than SparseLift’s,<sup>10</sup> although it

<sup>8</sup>EM-P-BiG-AMP was not told that the measurements were noiseless.

<sup>9</sup>See footnote 8.

<sup>10</sup>The SparseLift results in Fig. 3 agree with those in [8, Figure 1].

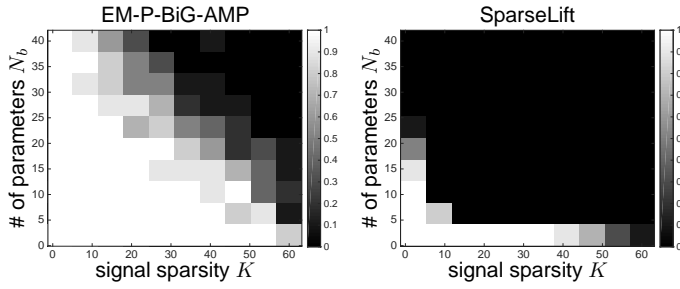


Fig. 3. Empirical success rate for *noiseless self-calibration* as a function of the number of calibration parameters  $N_b$  and the signal sparsity  $K$ . Results are averaged over 10 independent realizations.

was not close to the counting bound  $M \geq N_b + K$ , which lives just outside the boundaries of the figure. Still, the shape of EM-P-BiG-AMP's empirical phase-transition suggests successful recovery when  $M \gtrsim \alpha_1(N_b + K)$  for some  $\alpha_1$ , in contrast with SparseLift's empirical and theoretical [8] success condition of  $M \gtrsim \alpha_2 N_b K$  for some  $\alpha_2$ .

### C. Noisy CS with Parametric Matrix Uncertainty

Next we consider noisy compressive sensing with parametric matrix uncertainty, as described in Section I-A. Our goal is to recover a single,  $K$ -sparse,  $N_c$ -length signal  $\mathbf{c}$  from measurements  $\mathbf{y} = (\mathbf{A}^{(0)} + \sum_{i=1}^{N_b} b_i \mathbf{A}^{(i)})\mathbf{c} + \mathbf{w} \in \mathbb{R}^M$ , where  $\mathbf{b} = [b_1, \dots, b_{N_b}]^T$  are unknown calibration parameters and  $\mathbf{w}$  is AWGN. For our experiment,  $N_c = 256$ ,  $K = 10$ ,  $\mathbf{c}$  had i.i.d.  $\mathcal{N}(0, \nu^c)$  non-zero elements chosen uniformly at random with  $\nu^c = 1$ ,  $\mathbf{b}$  was i.i.d.  $\mathcal{N}(0, \nu^b)$  with  $\nu^b = 1$ ,  $\mathbf{A}^{(0)}$  was i.i.d.  $\mathcal{N}(0, 10)$ , and  $\{\mathbf{A}^{(i)}\}_{i=1}^{10}$  was i.i.d.  $\mathcal{N}(0, 1)$ . The noise variance  $\nu^w$  was adjusted to achieve an SNR  $\triangleq \|\mathbf{y} - \mathbf{w}\|_2^2 / \|\mathbf{w}\|_2^2$  of 40 dB.

We compared P-BiG-AMP and EM-P-BiG-AMP to i) the MMSE oracle that knows  $\mathbf{c}$ , ii) the MMSE oracle that knows  $\mathbf{b}$  and  $\text{support}(\mathbf{c})$ , and iii) the WSS-TLS approach from [9], which aims to solve the non-convex optimization problem

$$(\hat{\mathbf{b}}, \hat{\mathbf{c}}) = \arg \min_{\mathbf{b}, \mathbf{c}} \left\| \left( \mathbf{A}^{(0)} + \sum_{i=1}^{N_b} b_i \mathbf{A}^{(i)} \right) \mathbf{c} - \mathbf{y} \right\|_2^2 + \nu^w \|\mathbf{b}\|_2^2 + \lambda \|\mathbf{c}\|_1 \quad (123)$$

via alternating minimization. For WSS-TLS, we used oracle knowledge of  $\nu^w$ , oracle tuning of the regularization parameter  $\lambda$ , and code from the authors' website (with a trivial modification to facilitate arbitrary  $\mathbf{A}^{(i)}$ ). P-BiG-AMP used a Bernoulli-Gaussian prior with sparsity rate  $\xi = K/N_c$  and perfect knowledge of  $\nu^c$  and  $\nu^w$ , whereas EM-P-BiG-AMP learned the statistics  $[\xi, \nu^c, \nu^w]^T \triangleq \boldsymbol{\theta}$  from the observed data. Figure 4 shows that, for estimation of both  $\mathbf{b}$  and  $\mathbf{c}$ , P-BiG-AMP gave near-oracle NMSE performance for  $M/N \geq 0.2$ . Meanwhile, EM-P-BiG-AMP performed only slightly worse than P-BiG-AMP. In contrast, the NMSE performance of WSS-TLS was about 10 dB worse than P-BiG-AMP, and its "phase transition" occurred later, at  $M/N = 0.3$ .

### D. Totally Blind Deconvolution

We now consider recovering an unknown signal  $c_i$  and channel  $b_i$  from noisy observations  $y_i = z_i + w_i$  of their

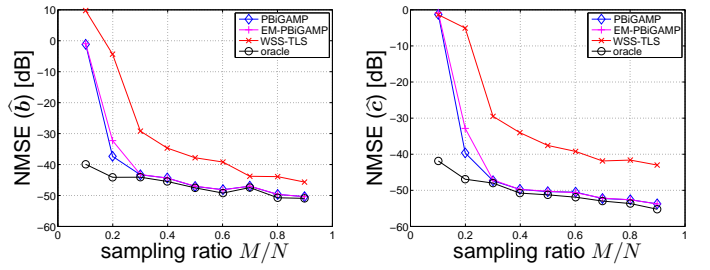


Fig. 4. Parameter estimation NMSE (left) and signal estimation NMSE (right) versus sampling ratio  $M/N$  for CS with parametric matrix uncertainty. Results are averaged over 10 independent realizations.

linear convolution  $z_i = b_i * c_i$ , where  $w_i \sim \text{i.i.d. } \mathcal{N}(0, \nu^w)$ . In particular, we consider the case of "totally blind deconvolution" from [49], where the signal contains zero-valued guard intervals of duration  $N_g \geq N_b - 1$  and period  $N_p > N_g$ , guaranteeing identifiability. Recalling the discussion of *joint channel-symbol estimation* in Section I-A, we see that a zero-valued guard allows the convolution outputs to be organized as  $\mathbf{Z} = \text{Conv}(\mathbf{b})\mathbf{C}$ , where  $\text{Conv}(\mathbf{b}) \in \mathbb{R}^{N_p \times (N_p - N_g)}$  is the linear convolution matrix with first column  $\mathbf{b}$ . For our experiment, we used an i.i.d.  $\mathcal{CN}(0, 1)$  channel  $\mathbf{b}$ , and two cases of i.i.d. signal  $\mathbf{c}$ : Gaussian  $c_j \sim \mathcal{CN}(0, 1)$  and equiprobable QPSK (i.e.,  $c_j \in \{1, j, -1, -j\}$ ). Also, we used guard period  $N_p = 256$ , guard duration  $N_g = 64$ , channel length  $N_b = 63$ , and  $L = 3$  signal periods.

We compared P-BiG-AMP to i) the known-symbol and known-channel MMSE oracles and ii) the cross-relation (CR) method [50], which is known to perform close to the Cramer-Rao lower bound [50]. In particular, we used CR for blind symbol estimation, then (in the QPSK case) de-rotated and quantized the blind symbol estimates, and finally performed maximum-likelihood channel estimation assuming perfect (quantized) symbols. Figure 5 shows that, with both Gaussian and QPSK symbols, P-BiG-AMP outperformed the CR method by about 5 dB in the SNR domain. Moreover, by exploiting the QPSK constellation, both methods were able to achieve oracle-grade NMSE( $\hat{\mathbf{b}}$ ) at high SNR.

### E. Matrix Compressive Sensing

Finally, we consider the problem of *matrix compressive sensing*, as described in Section I-A and further discussed in Section IV-D. Our goal was to jointly recover a low rank matrix  $\mathbf{L} = \mathbf{B}^T \mathbf{C}_1 \in \mathbb{C}^{100 \times 100}$  and a sparse outlier matrix  $\mathbf{S} = \mathbf{C}_2 \in \mathbb{C}^{100 \times 100}$  from  $M$  noiseless linear measurements of their sum, i.e.,  $\{z_m\}_{m=1}^M$  in (3). For our experiment, the sparse outliers were drawn with amplitudes uniformly distributed on  $[-10, 10]$  and uniform random phases, similar to [14, Figure 2]. But unlike [14, Figure 2], the sensing matrices  $\{\Phi_m\}$  were sparse, with  $K = 50$  i.i.d.  $\mathcal{CN}(0, 1)$  non-zero entries drawn uniformly at random.

We compare the recovery performance of EM-P-BiG-AMP to the convex formulation known as *compressive principal components pursuit* (CPCP) [14], i.e.,

$$\arg \min_{\mathbf{L}, \mathbf{S}} \|\mathbf{L}\|_* + \lambda \|\mathbf{S}\|_1 \text{ s.t. } z_m = \text{tr}\{\Phi_m^T (\mathbf{L} + \mathbf{S})\} \quad \forall m, \quad (124)$$

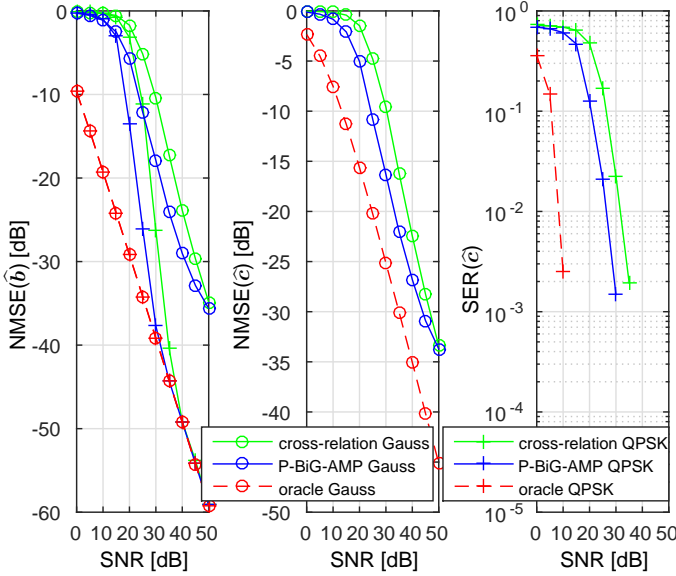


Fig. 5. Channel estimation NMSE (left), Gaussian-symbol estimation NMSE (center), and QPSK symbol error rate (right) versus SNR for *totally blind deconvolution*. Results are averaged over 500 independent realizations.

which we solved with TFOCS using a continuation scheme. In accordance with [14, Theorem 2.1], we used  $\lambda = 1/10$  in (124). EM-P-BiG-AMP learned the variance of the entries in  $C_1$ , the sparsity and non-zero variance of  $C_2$ , and the additive AWGN variance.<sup>11</sup> Although EM-P-BiG-AMP was given knowledge of the true rank  $R$ , we note that an unknown rank could be accurately estimated using the scheme proposed for BiG-AMP in [20, Sec. V-B2] and tested for the RPCA application in [21, Sec. III-F2].

Figure 6 shows the empirical success rate of EM-P-BiG-AMP and CPCP versus  $R$  (i.e., the rank of  $L$ ) and  $\xi = K/100^2$  (i.e., the sparsity rate of  $S$ ) for three fixed values of  $M$  (i.e., the number of measurements). Each point is the average of 10 independent trials, with success defined as  $\|L - \hat{L}\|_F^2 / \|L\|_F^2 < -60$  dB. Figure 6 shows that, for the three tested values of  $M$ , EM-P-BiG-AMP exhibited a sharp phase-transition that was significantly better than that of CPCP.<sup>12</sup> In fact, EM-P-BiG-AMP's phase transition is not far from the counting bound  $M \geq R(200 - R) + \xi 100^2$ , shown by the red curves in Fig. 6.

Figure 7 shows the corresponding  $\log_{10}$ (average runtime) versus rank  $R$  and sparsity rate  $\xi$  at  $M = 10000$  measurements. Runtimes were averaged over 10 *successful* trials; locations  $(R, \xi)$  with any unsuccessful trials are shown in white. The figure shows that EM-P-BiG-AMP's average runtimes were faster TFOCS's throughout the region that both algorithms were successful. The runtimes for other values of  $M$  (not shown) were similar.

## VI. CONCLUSION

We proposed P-BiG-AMP, a scheme to estimate the parameters  $\mathbf{b} = [b_1, \dots, b_{N_b}]^T$  and  $\mathbf{c} = [c_1, \dots, c_{N_c}]^T$  of the

<sup>11</sup>See footnote 8.

<sup>12</sup>The CPCP results in Fig. 6 are in close agreement with those in [14, Figure 2], even though the latter correspond to real-valued and dense  $\Phi_m$ .

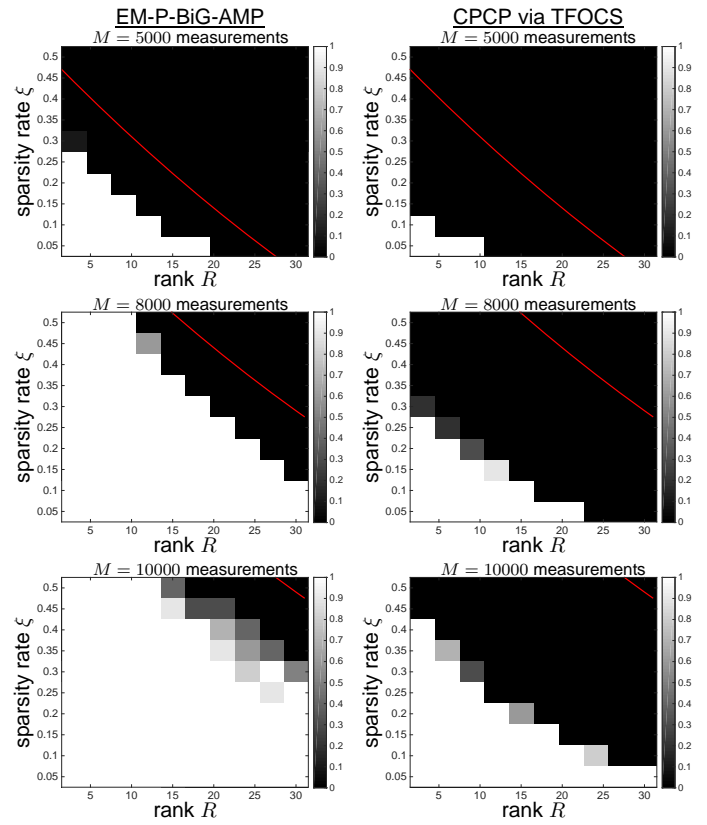


Fig. 6. Empirical success rate for noiseless *matrix compressive sensing* as a function of rank  $R$  and outlier sparsity rate  $\xi$  for  $M = 5000$  (top),  $M = 8000$  (middle), and  $M = 10000$  (bottom) measurements. The left column shows EM-P-BiG-AMP and the right column shows CPCP solved using TFOCS. All results are averaged over 10 independent realizations. Points above the red curve are infeasible due to the counting bound, as described in the text.

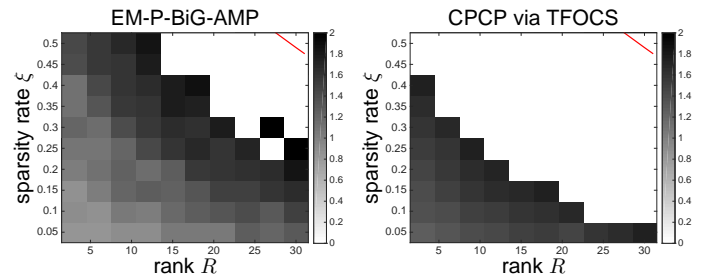


Fig. 7.  $\log_{10}$ (average runtime), in seconds, for noiseless *matrix compressive sensing* as a function of rank  $R$  and outlier sparsity rate  $\xi$  for  $M = 10000$  measurements. Runtimes were averaged over 10 successful trials; locations  $(R, \xi)$  with any unsuccessful trials are shown in white.

parametric bilinear form  $z_m = \sum_{i=0}^{N_b} \sum_{j=0}^{N_c} b_i z_m^{(i,j)} c_j$  from noisy measurements  $\{y_m\}_{m=1}^M$ , where  $y_m$  and  $z_m$  are related through an arbitrary likelihood function and  $z_m^{(i,j)}$ ,  $b_0, c_0$  are known. Our approach treats  $b_i$  and  $c_j$  as random variables and  $z_m^{(i,j)}$  as an i.i.d. Gaussian tensor in order to derive a tractable simplification of the sum-product algorithm in the large-system limit, generalizing the bilinear AMP algorithms in [20], [22]. We also proposed an EM extension that learns the statistical parameters of the priors on  $b_i$ ,  $c_j$ , and  $y_m|z_m$ . Numerical experiments suggest that our schemes yield significantly better phase transitions than several recently proposed convex and non-convex approaches to self-calibration, blind

deconvolution, CS under matrix uncertainty, and matrix CS, while being competitive (or faster) in runtime.

## REFERENCES

- [1] J. T. Parker, "Approximate message passing algorithms for generalized bilinear inference," Ph.D. dissertation, The Ohio State University, Columbus, OH, Aug. 2014.
- [2] E. J. Candès and Y. Plan, "Matrix completion with noise," *Proc. IEEE*, vol. 98, no. 6, pp. 925–936, Jun. 2010.
- [3] E. J. Candès, X. Li, Y. Ma, and J. Wright, "Robust principal component analysis?" *J. ACM*, vol. 58, no. 3, p. 11, May 2011.
- [4] V. Chandrasekaran, S. Sanghavi, P. A. Parrilo, and A. S. Willsky, "Rank-sparsity incoherence for matrix decomposition," *SIAM J. Optim.*, vol. 21, pp. 572–596, 2011.
- [5] Z. Zhou, J. Wright, X. Li, E. J. Candès, and Y. Ma, "Stable principal component pursuit," in *Proc. IEEE Int. Symp. Inform. Thy.*, Austin, TX, Jun. 2010.
- [6] R. Rubinstein, A. Bruckstein, and M. Elad, "Dictionaries for sparse representation modeling," *Proceedings of the IEEE*, vol. 98, no. 6, pp. 1045–1057, 2010.
- [7] D. D. Lee and H. S. Seung, "Algorithms for non-negative matrix factorization," in *Proc. Neural Inform. Process. Syst. Conf.*, 2001, pp. 556–562.
- [8] S. Ling and T. Strohmer, "Self-calibration and biconvex compressive sensing," *arXiv:1501.06864v2*, 2015.
- [9] H. Zhu, G. Leus, and G. B. Giannakis, "Sparsity-cognizant total least-squares for perturbed compressive sampling," *IEEE Trans. Signal Process.*, vol. 59, no. 5, pp. 2002–2016, May 2011.
- [10] J. T. Parker and P. Schniter, "Parametric bilinear generalized approximate message passing," *Supplementary material for review*, 2015.
- [11] A. E. Waters, A. C. Sankaranarayanan, and R. G. Baraniuk, "SpARCS: Recovering low-rank and sparse matrices from compressive measurements," in *Proc. Neural Inform. Process. Syst. Conf.*, 2011, pp. 1089–1097.
- [12] E. J. Candès and Y. Plan, "Tight oracle inequalities for low-rank matrix recovery from a minimal number of noisy random measurements," *IEEE Trans. Inform. Theory*, vol. 57, no. 4, pp. 2342–2359, 2011.
- [13] A. Agarwal, S. Negahban, and M. J. Wainwright, "Matrix decomposition via convex relaxation: Optimal rates in high dimensions," *Ann. Statist.*, vol. 40, no. 2, pp. 1171–1197, 2012.
- [14] J. Wright, A. Ganesh, K. Min, and Y. Ma, "Compressive principal component pursuit," *Inform. Inference*, vol. 2, no. 1, pp. 32–68, 2013.
- [15] U. S. Kamilov, V. K. Goyal, and S. Rangan, "Message-passing dequantization with applications to compressed sensing," *IEEE Trans. Signal Process.*, vol. 60, no. 12, pp. 6270–6281, Dec. 2012.
- [16] A. K. Fletcher, S. Rangan, L. R. Varshney, and A. Bhargava, "Neural reconstruction with approximate message passing (NeuRAMP)," in *Proc. Neural Inform. Process. Syst. Conf.*, 2011.
- [17] P. Schniter and S. Rangan, "Compressive phase retrieval via generalized approximate message passing," *IEEE Trans. Signal Process.*, vol. 63, no. 4, pp. 1043–1055, Feb. 2015, (see also *arXiv:1405.5618*).
- [18] A. Montanari, "Graphical models concepts in compressed sensing," in *Compressed Sensing: Theory and Applications*, Y. C. Eldar and G. Kutyniok, Eds. Cambridge Univ. Press, 2012.
- [19] S. Rangan, "Generalized approximate message passing for estimation with random linear mixing," in *Proc. IEEE Int. Symp. Inform. Thy.*, Aug. 2011, pp. 2168–2172, (full version at *arXiv:1010.5141*).
- [20] J. T. Parker, P. Schniter, and V. Cevher, "Bilinear generalized approximate message passing—Part I: Derivation," *IEEE Trans. Signal Process.*, vol. 62, no. 22, pp. 5839–5853, Nov. 2014, (See also *arXiv:1310.2632*).
- [21] —, "Bilinear generalized approximate message passing—Part II: Applications," *IEEE Trans. Signal Process.*, vol. 62, no. 22, pp. 5854–5867, Nov. 2014, (See also *arXiv:1310.2632*).
- [22] Y. Kabashima, F. Krzakala, M. Mezard, A. Sakata, and L. Zdeborova, "Phase transitions and sample complexity in Bayes-optimal matrix factorization," *arXiv:1402.1298*, 2014.
- [23] A. Dempster, N. M. Laird, and D. B. Rubin, "Maximum-likelihood from incomplete data via the EM algorithm," *J. Roy. Statist. Soc.*, vol. 39, pp. 1–17, 1977.
- [24] F. Krzakala, M. Mézard, F. Sausset, Y. Sun, and L. Zdeborová, "Probabilistic reconstruction in compressed sensing: Algorithms, phase diagrams, and threshold achieving matrices," *J. Stat. Mech.*, vol. P08009, 2012.
- [25] J. P. Vila and P. Schniter, "Expectation-maximization Gaussian-mixture approximate message passing," *IEEE Trans. Signal Process.*, vol. 61, no. 19, pp. 4658–4672, Oct. 2013.
- [26] U. S. Kamilov, S. Rangan, A. K. Fletcher, and M. Unser, "Approximate message passing with consistent parameter estimation and applications to sparse learning," *IEEE Trans. Inform. Theory*, vol. 60, no. 5, pp. 2969–2985, May 2014.
- [27] R. Gribonval, G. Chardon, and L. Daudet, "Blind calibration for compressed sensing by convex optimization," in *Proc. IEEE Int. Conf. Acoust. Speech & Signal Process.*, 2012, pp. 2713–2716.
- [28] C. Bilen, G. Puy, and R. Gribonval, "Convex optimization approaches for blind sensor calibration using sparsity," *IEEE Trans. Signal Process.*, vol. 62, no. 18, pp. 4847–4856, 2014.
- [29] C. Schülke, F. Caltagirone, F. Krzakala, and L. Zdeborová, "Blind calibration in compressed sensing using message passing algorithms," in *Proc. Neural Inform. Process. Syst. Conf.*, 2014.
- [30] P. Schniter, "A message-passing receiver for BICM-OFDM over unknown clustered-sparse channels," *IEEE J. Sel. Topics Signal Process.*, vol. 5, no. 8, pp. 1462–1474, Dec. 2011.
- [31] U. S. Kamilov, A. Bourquard, E. Bostan, and M. Unser, "Autocalibrated signal reconstruction from linear measurements using adaptive GAMP," in *Proc. IEEE Int. Conf. Acoust. Speech & Signal Process.*, 2013, pp. 5925–5928.
- [32] M. S. Asif, W. Mantzel, and J. Romberg, "Random channel coding and blind deconvolution," in *Proc. Allerton Conf. Commun. Control Comput.*, 2009, pp. 1021–1025.
- [33] A. Ahmed, B. Recht, and J. Romberg, "Blind deconvolution using convex programming," *arXiv:1211.5608*, 2012.
- [34] C. Hegde and R. G. Baraniuk, "Sampling and recovery of pulse streams," *IEEE Trans. Signal Process.*, vol. 59, no. 14, pp. 1505–1517, 2011.
- [35] S. Choudhary and U. Mitra, "Fundamental limits of blind deconvolution Part I: Ambiguity kernel," *arXiv:1411.3810*, 2014.
- [36] —, "Fundamental limits of blind deconvolution Part II: Sparsity-ambiguity trade-offs," *arXiv:1503.03184*, 2015.
- [37] —, "Identifiability scaling laws in bilinear inverse problems," *arXiv:1402.2637*, 2014.
- [38] T. Zhou and D. Tao, "Godec: Randomized low-rank & sparse matrix decomposition in noisy case," in *Proc. Int. Conf. Mach. Learning*, 2011.
- [39] A. Kyrillidis and V. Cevher, "Matrix ALPs: Accelerated low rank and sparse matrix reconstruction," *arXiv:1203.3864*, 2012.
- [40] A. Aravkin, S. Becker, V. Cevher, and P. Olsen, "A variational approach to stable principal component pursuit," in *Proc. Conf. Uncertainty Artificial Intell.*, 2014.
- [41] J. Pearl, *Probabilistic Reasoning in Intelligent Systems*. San Mateo, CA: Morgan Kaufman, 1988.
- [42] F. R. Kschischang, B. J. Frey, and H.-A. Loeliger, "Factor graphs and the sum-product algorithm," *IEEE Trans. Inform. Theory*, vol. 47, pp. 498–519, Feb. 2001.
- [43] G. F. Cooper, "The computational complexity of probabilistic inference using Bayesian belief networks," *Artificial Intelligence*, vol. 42, pp. 393–405, 1990.
- [44] K. P. Murphy, Y. Weiss, and M. I. Jordan, "Loopy belief propagation for approximate inference: An empirical study," in *Proc. Uncertainty Artif. Intell.*, 1999, pp. 467–475.
- [45] A. Javanmard and A. Montanari, "State evolution for general approximate message passing algorithms, with applications to spatial coupling," *Inform. Inference*, vol. 2, no. 2, pp. 115–144, 2013.
- [46] S. Rangan, P. Schniter, and A. Fletcher, "On the convergence of generalized approximate message passing with arbitrary matrices," in *Proc. IEEE Int. Symp. Inform. Thy.*, Jul. 2014, pp. 236–240, (full version at *arXiv:1402.3210*).
- [47] J. Vila, P. Schniter, S. Rangan, F. Krzakala, and L. Zdeborová, "Adaptive damping and mean removal for the generalized approximate message passing algorithm," in *Proc. IEEE Int. Conf. Acoust. Speech & Signal Process.*, 2015.
- [48] S. Rangan, P. Schniter, J. T. Parker, J. Ziniel, J. Vila, M. Borgerding *et al.*, "GAMPmatlab," <https://sourceforge.net/projects/gampmatlab/>.
- [49] J. H. Manton and W. D. Neumann, "Totally blind channel identification by exploiting guard intervals," *Syst. Control Lett.*, vol. 48, pp. 113–119, 2003.
- [50] Y. Hua, "Fast maximum likelihood for blind identification of multiple FIR channels," *IEEE Trans. Signal Process.*, vol. 44, pp. 661–672, 1996.